

1

2 **Determination of vadose and saturated-zone nitrate lag times using long-** 3 **term groundwater monitoring data and statistical machine learning**

4 Martin J. Wells^{1,3}, Troy E. Gilmore^{2,3}, Natalie Nelson^{4,5}, Aaron Mittelstet³, J.K. Böhlke⁶,

5 ¹currently at Natural Resources Conservation Service, Redmond, OR, 97756, USA

6 ²Conservation and Survey Division - School of Natural Resources, University of Nebraska, Lincoln, NE, 68583, USA

7 ³Biological Systems Engineering, University of Nebraska, Lincoln, NE, 68583, USA

8 ⁴Biological and Agricultural Engineering, North Carolina State University, Raleigh, NC, 27695, USA

9 ⁵Center for Geospatial Analytics, North Carolina State University, Raleigh, NC, 27695, USA

10 ⁶U.S. Geological Survey, Reston, VA, 20192, USA

11 *Correspondence to:* Troy E. Gilmore (gilmore@unl.edu)

12 **Abstract.** In this study, we explored the use of statistical machine learning and long-term groundwater nitrate monitoring data to
13 estimate vadose-zone and saturated-zone lag times in an irrigated alluvial agricultural setting. Unlike most previous statistical
14 machine learning studies that sought to predict groundwater nitrate concentrations within aquifers, the focus of this study was to
15 leverage available groundwater nitrate concentrations and other environmental variables to determine mean regional vertical
16 velocities (transport rates) of water and solutes in the vadose zone and saturated zone (3.50 m/year and 3.75 m/year, respectively).
17 The statistical machine learning results are consistent with two contrasting primary recharge processes in this Western Nebraska
18 aquifer: (1) diffuse recharge from irrigation and precipitation across the landscape, and (2) focused recharge from leaking irrigation
19 conveyance canals. The vadose-zone mean velocity yielded a mean recharge rate (0.46 m/year) consistent with previous estimates
20 from groundwater age-dating in shallow wells (0.38 m/year). The saturated zone mean velocity yielded a recharge rate (1.31
21 m/year) that was more consistent with focused recharge from leaky irrigation canals, as indicated by previous results of
22 groundwater age-dating in intermediate-depth wells (1.22 m/year). Collectively, the statistical machine-learning model results are
23 consistent with previous observations of relatively high-water fluxes and short transit times for water and nitrate in the primarily
24 oxic aquifer. Partial dependence plots from the model indicate a sharp threshold where high groundwater nitrate concentrations
25 are mostly associated with total travel times of seven years or less, possibly reflecting some combination of recent management
26 practices and a tendency for nitrate concentrations to be higher in diffuse infiltration recharge than in canal leakage water.
27 Limitations to the machine learning approach include potential non-uniqueness of different transport rate combinations when
28 comparing model performance and highlight the need to corroborate statistical model results with a robust conceptual model and
29 complementary information such as groundwater age.

30

31

32

33

34

35

36 1 Introduction

37 Nitrate is a common contaminant of groundwater and surface water that can affect drinking water quality and ecosystem
38 health. Responses of aquatic resources to changes in nitrate loading can be complicated by uncertainties related to rates and
39 pathways of nitrate transport from sources to receptors. Lag times for movement of non-point source nitrate contamination through
40 the subsurface are widely recognized (Böhlke, 2002; Meals et al., 2010; Puckett et al., 2011; Van Meter and Basu, 2017) but
41 difficult to measure. Vadose (unsaturated zone) and groundwater (saturated zone) lag times are of critical importance for
42 monitoring, regulating, and managing the transport of contaminants in groundwater. However, transport time-scales are often
43 generalized due to coarse spatial and temporal resolution in data available for groundwater systems impacted by agricultural
44 activities (Gilmore et al., 2016; Green et al., 2018; Puckett et al., 2011), resulting in a simplified groundwater management
45 approach. Regulators and stakeholders in agricultural landscapes are increasingly in need of more precise and local lag time
46 information to better evaluate and apply regulations and best management practices for the reduction of groundwater nitrate
47 concentrations (e.g., Eberts et al., 2013).

48 Field-based studies of lag times commonly use expensive groundwater age-dating techniques and/or vadose-zone
49 sampling to estimate nitrate transport rates moving into and through aquifers (Böhlke et al., 2002, 2007; Böhlke and Denver, 1995;
50 Browne and Guldan, 2005; Kennedy et al., 2009; McMahon et al., 2006; Morgenstern et al., 2015; Turkeltaub et al., 2016; Wells
51 et al., 2018). Detailed process-based modelling studies focused on lag times require complex numerical models combined with
52 spatially intensive and/or costly hydrogeological observations (Ilampooranan et al., 2019; Rossman et al., 2014; Russoniello et al.,
53 2016). Thus, efficient but locally-applicable modelling approaches are needed (Green et al., 2018; Liao et al., 2012; Van Meter
54 and Basu, 2015). In this study, an alternative data-driven approach (Random Forest Regression) leverages existing long-term
55 groundwater nitrate concentration (referred to as $[\text{NO}_3^-]$ hereafter) data and easily accessible environmental data to estimate vadose
56 and saturated-zone vertical velocities (transport rates) for the determination of subsurface lag times.

57 Statistical machine learning methods, including Random Forest, have been used successfully for modelling $[\text{NO}_3^-]$
58 distribution in aquifers (Anning et al., 2012; Juntakut et al., 2019; Knoll et al., 2020; Nolan et al., 2014; Ouedraogo et al., 2017;
59 Rodriguez-Galiano et al., 2014; Rahmati et al., 2019; Vanclooster et al., 2020; Wheeler et al., 2015), but there has not been robust
60 analysis of model capabilities for estimating vadose and/or saturated-zone lag times. Proxies for lag time, such as well screen
61 depth, have been used as predictors in Random Forest models (Nolan et al., 2014; Wheeler et al., 2015). Decadal lag times have
62 been suggested from using time-averaged nitrogen inputs as predictors (e.g., 1978-1990 inputs vs 1992-2006 inputs) and by
63 comparing their relative importance in the model (Wheeler et al., 2015). Application of similar machine learning methods
64 suggested groundwater age could be used as a predictor to improve model performance (Ransom et al., 2017). Hybrid models,
65 using both mechanistic models and machine learning, have also sought to integrate vertical transport model parameters and outputs
66 to evaluate nitrate-related predictors, including vadose-zone travel times (Nolan et al., 2018).

67 The objective of this study is to test a data-driven approach for estimating vadose and saturated-zone transport rates and
68 lag times for an intensively monitored alluvial aquifer in western Nebraska (Böhlke et al., 2007; Verstraeten et al., 2001a, 2001b;
69 Wells et al., 2018). Results are compared to the hydrogeologic, mechanistic understanding from previous groundwater studies to
70 determine strengths and weaknesses of the approach as (1) a stand-alone technique, or (2) as an exploratory analysis to guide or
71 complement more complex physical-based models or intensive hydrogeologic field investigations.

72 2 Methods

73 2.1 Site Description

74 The Dutch Flats study area is located in the western Nebraska counties of Scotts Bluff and Sioux (Fig. 1). The North
75 Platte River delivers large quantities of water for crop irrigation in this region and runs along the southern portion of this study
76 area. Irrigation water is diverted from the North Platte River into three major canals (Mitchell-Gering, Tri-State, and Interstate
77 Canals) that feed a network of minor canals. Several previous Dutch Flats area studies have investigated groundwater
78 characteristics and provided thorough site descriptions of the semi-arid region (Babcock et al., 1951; Böhlke et al., 2007;
79 Verstraeten et al., 2001a, 2001b; Wells et al., 2018). The Dutch Flats area overlies an alluvial aquifer characterized by
80 unconsolidated deposits of predominantly sand and gravel, with the aquifer base largely consisting of consolidated deposits of the
81 Brule, Chadron, or Lance Formation (Verstraeten et al., 1995) (Fig. 2). Irrigation water not derived from the North Platte River is
82 typically pumped from the alluvial aquifer, or water-bearing units of the Brule Formation.

83 The total area of the Dutch Flats study area is roughly 540 km², of which approximately 290 km² (53.5%) is agricultural
84 land (cultivated crops and pasture). Most agricultural land is concentrated south of the Interstate Canal (Homer et al., 2015). Due
85 to the combination of intense agriculture and low annual precipitation, producers in Dutch Flats rely on a network of irrigation
86 canals to supply water to the region. From 1908 to 2016, mean precipitation of 390 mm was measured at the nearby Western
87 Regional Airport in Scottsbluff, NE (NOAA, 2017).

88 While some groundwater is withdrawn for irrigation, and some irrigated acres in the study area are classified as
89 commingled (groundwater and surface water source), Scotts Bluff County irrigation is mostly from surface water sources.
90 Estimates determined every five years suggest surface water provided between 76.8% to 98.6% of the total water withdrawals from
91 1985 to 2015, or about 92% on average (Dieter et al., 2018). Canals transport water from the North Platte River to fields throughout
92 the study area, most of which are downgradient (south) of the Interstate Canal. Mitchell-Gering, Tri-State, and Interstate Canals
93 are the major canals in Dutch Flats, with the latter holding the largest water right of 44.5 m³/s (NEDNR, 2009). Leakage from
94 these canals provides a source of artificial groundwater recharge. Previous studies estimate the leakage potential of canals in the
95 region results in as much as 40% to 50% of canal water being lost during conveyance (Ball et al., 2006; Harvey and Sibray, 2001;
96 Hobza and Andersen, 2010; Luckey and Cannia, 2006). Leakage estimates from a downstream section of the Interstate Canal
97 (extending to the east of the study area; Hobza and Andersen (2010)) suggest fluxes ranging from 0.08 to 0.7 m day⁻¹ through the
98 canal bed. Assuming leakage of 0.39 m day⁻¹ over the Interstate Canal bed area (16.8 m width x 55.5 km length) within Dutch
99 Flats yields 4.1 x 10⁵ m³ day⁻¹ of leakage. Applied over an on-average 151-day operation period (USBR, 2018), leakage from
100 Interstate Canal alone could approach 6.1 x 10⁷ m³ annually, or about 29% of the annual volume of precipitation in the Dutch Flats
101 area.

102 A 1990s study investigated both spatial and temporal influences from canals in the Dutch Flats area (Verstraeten et al.,
103 2001a, 2001b), with results later synthesized by Böhlke et al. (2007). Canals were found to dilute groundwater [NO₃⁻] locally with
104 low-[NO₃⁻] (e.g., [NO₃⁻] < 0.06 mg N L⁻¹ in 1997) surface water during irrigation season. ³H/³He age-dating was used to determine
105 apparent groundwater ages and recharge rates. It was noted that wells near canals displayed evidence of high recharge rates
106 influenced by local canal leakage. Data from wells far from the canals indicated that shallow groundwater was more likely
107 influenced by local irrigation practices (i.e., furrows in fields), while deeper groundwater was impacted by both localized irrigation
108 and canal leakage (Böhlke et al., 2007). Shallow groundwater in the Dutch Flats area has hydrogen and oxygen stable isotopic
109 compositions consistent with surface water sources (i.e., North Platte River and associated canals), indicating that most
110 groundwater intercepted by the monitoring well network has been affected by surface-water irrigation recharge (Böhlke et al.,
111 2007; Cherry et al., 2020).

112 The Dutch Flats area is within the North Platte Natural Resources District (NPNRD), one of 23 groundwater management
113 districts in Nebraska tasked with, among other functions, improving water quality and quantity. The NPNRD has a large monitoring
114 well network consisting of 797 wells, 327 of which are nested. Nested well clusters are drilled and constructed such that screen
115 intervals represent (1) “shallow” groundwater intersecting the water table (length of screened interval = 6.1 m), (2) “intermediate”
116 groundwater from mid-aquifer depths (length of screened interval = 1.5 m), and deep groundwater near the base of the unconfined
117 aquifer (length of screened interval = 1.5 m). Depending on well location within the Dutch Flats area, depths of the water table and
118 base of aquifer are highly variable, such that shallow, intermediate, and deep wells can have overlapping ranges of depths below
119 land surface (Fig. 2).

120 Influenced by both regulatory and economic incentives, the Dutch Flats area has undergone a notable shift in irrigation
121 practices in the last two decades. From 1999 to 2017, center pivot irrigated area has increased by approximately 270%, from
122 roughly 3,830 hectares to 14,253 hectares, or from 13% to 49% of the total agricultural land area, respectively. The majority of
123 this shift in technology has occurred on fields previously under furrow irrigation. Conventional furrow irrigation has an estimated
124 potential application efficiency (“measure of the fraction of the total volume of water delivered to the farm or field to that which
125 is stored in the root zone to meet the crop evapotranspiration needs,” per Irmak et al. (2011)) of 45% to 65%, compared to center
126 pivot sprinklers at 75% to 85% (Irmak et al., 2011). Based on improved irrigation efficiency (between 10-40%), average
127 precipitation throughout growing season (29.5 cm for 15 April to 13 October (Yonts, 2002)), and average water requirements for
128 corn (69.2 cm (Yonts, 2002)), converting furrow irrigated fields to center pivot over the aforementioned 14,253 hectares could
129 represent a difference of $1 \times 10^7 \text{ m}^3$ to $6 \times 10^7 \text{ m}^3$ in water applied. Those (roughly approximated) differences in water volumes are
130 equivalent to 6-28% of average annual precipitation applied over the Dutch Flats area, suggesting the change in irrigation practice
131 does have potential to alter the water balance in the area.

132 The hypothesis of lower recharge due to changes in irrigation technology was investigated by Wells et al. (2018) by
133 comparing samples collected in 1998 and 2016. Sample sites were selected based on a well’s proximity to fields that observed a
134 conversion in irrigation practices (i.e., furrow irrigation to center pivot) between the two collection periods. While mean recharge
135 rate was not significantly different, a lower recharge rate was indicated by data from 88% of the wells. Long-term Dutch Flats
136 $[\text{NO}_3^-]$ trends were also assessed in the study, suggesting decreasing trends (though statistically insignificant) from 1998 to 2016
137 throughout the Dutch Flats area, and nitrogen isotopes of nitrate indicated little change in biogeochemical processes. For additional
138 background, Wells et al., (2018) provides a more in-depth analysis of recent $[\text{NO}_3^-]$ trends in this region (see also, Fig. S1A, which
139 shows the nitrate data used in the present study).

140 As in other agricultural areas, nitrate in Dutch Flats groundwater is dependent on nitrogen loading at the land surface, rate
141 of leaching below crop root zones, rate of nitrate transport through the vadose and saturated zones, dilution from focused recharge
142 in the vicinity of canals, rate of discharge from the aquifer (whether from pumping or discharge to surface water bodies), and rates
143 of nitrate reduction (primarily denitrification) in the aquifer. Based on nitrogen and oxygen isotopes in nitrate and redox conditions
144 observed in previous studies, denitrification likely has a relatively minor or localized influence on groundwater nitrate in the Dutch
145 Flats area (Wells et al., 2018). Evidence of denitrification (from dissolved gases and isotopes (Böhlke et al., 2007, Wells et al.
146 2018)) was mostly limited to some of the deepest wells near the bottom of the aquifer. Leakage of low-nitrate water in the major
147 canals causes nitrate dilution in the groundwater (i.e., relatively little nitrate addition, at least from the upgradient canals).
148 Additional isotope data might be useful for documenting temporal shifts in recharge sources, or irrigation return flows to the river;
149 however, it is difficult to know exactly the location or size of the contributing area for each well, especially the deeper ones.

150 Other long-term changes to the landscape were evaluated by Wells et al. (2018) and included statistically significant
151 reductions in mean fertilizer application rates (1987–1999 vs. 2000–2012) and volume of water diverted into the Interstate Canal

152 (1983–1999 vs. 2000–2016), while a significant increase in area of planted corn occurred (1983–1999 vs. 2000–2016).
153 Precipitation was also evaluated, and though the mean has decreased over a similar time period, the trend was not statistically
154 significant.

155 2.2 Statistical Machine Learning Modelling Framework

156 Statistical machine learning uses algorithms to assess and identify complex relationships between variables. Learned
157 relations can be used to uncover nonlinear trends in data that might otherwise be overshadowed when using simple regression
158 techniques (Hastie et al., 2009). In this study we used Random Forest Regression, where Random Forests are created by combining
159 hundreds of unskilled regression trees into one model ensemble, or “forest”, which collectively produce skilled and robust
160 predictions (Breiman, 2001). Predictors used in the model represent site-specific explanatory variables (e.g., precipitation, vadose-
161 zone thickness, depth to bottom of screen, etc.) that may impact the response variable, groundwater [NO₃⁻]. Additionally, as
162 described in detail in Section 2.5, we estimated a range of total travel times (from land surface to the point of sampling) at each of
163 the wells by varying vadose and saturated-zone transport rates. The relative importance of total travel time as a predictor variable
164 was ultimately used to identify an optimal travel time and model.

165 2.3 Random Forest Application

166 Random Forest regression models of groundwater [NO₃⁻] were developed using five-fold cross validation (Hastie et al.,
167 2009), where four folds were used to build the model (training data), and one fold was held out (testing data). The maximum and
168 minimum of the [NO₃⁻] and each predictor were determined and placed into each fold for training models to eliminate the potential
169 for extrapolation during validation. Each fold was used as training data four times, and testing data once. This process was repeated
170 five times to create a total of 25 models, similar to the approach used by Nelson et al. (2018). The four folds designated to build
171 the model underwent a nested five-fold cross validation, as specified in the *trainControl* function within the *caret* (Classification
172 and Regression Training) R package (Kuhn, 2008; R Core Team, 2017). Functions in *caret* were used to train the Random Forest
173 models.

174 To evaluate model performance, Nash-Sutcliffe Efficiency (NSE), permutation importance, and partial dependence were
175 quantified. NSE indicates the degree to which observed and predicted values deviate from a 1:1 line, and ranges from negative
176 infinity to 1 (Nash and Sutcliffe, 1970).

$$177 \text{NSE} = 1 - \frac{\left[\sum_{i=1}^n (Y_i^{obs} - Y_i^{pred})^2 \right]}{\left[\sum_{i=1}^n (Y_i^{obs} - Y^{mean})^2 \right]}, \quad (1)$$

178 where n is the number of observations, Y_i^{obs} is the i^{th} observation of the response variable ([NO₃⁻]), Y_i^{pred} is the i^{th} prediction from
179 the Random Forest model, and Y^{mean} is the mean of observations i through n . Values from negative infinity to 0 suggest the mean
180 of the observed [NO₃⁻] would serve as a better predictor than the model. When NSE = 0, model predictions are as accurate as that
181 of a model with only the mean observed [NO₃⁻] as a predictor. From 0, larger NSE values indicate a model’s predictive ability
182 improves, until NSE = 1, where observations and predictions are equal. NSE was calculated for both the training and testing data.

183 For each tree, a random bootstrapped sample (i.e., data randomly pulled from the dataset, sampled with replacement) is
184 extracted from the dataset (Efron, 1979), as well as a random subset of predictors to consider fitting at each split. Thus, each tree
185 is grown from a bootstrap sample and random subset of predictors, making trees random and grown independent of the others.
186 Observations not used as bootstrap samples are termed out-of-bag (OOB) data.

187 When building a tree, all [NO₃⁻] from the bootstrap sample are categorized into terminal nodes, such that each node is
188 averaged and yields a predicted [NO₃⁻]. The performance and mean squared error (MSE) of a Random Forest model is evaluated

189 by comparing the observed $[\text{NO}_3^-]$ of the OOB data to the average predicted $[\text{NO}_3^-]$ from the forest. OOB data from the training
190 dataset may be used to evaluate both permutation importance, referred to in the rest of this text as variable importance, and partial
191 dependence. Variable importance uses percent increase in mean squared error ($\%_{\text{incMSE}}$) to describe predictive power of each
192 predictor in the model (Jones and Linder, 2015). During this process, a single predictor is permuted, or shuffled, in the dataset.
193 Therefore, each observed $[\text{NO}_3^-]$ has the same relationship between itself and all predictors, except one permuted variable. The
194 $\%_{\text{incMSE}}$ of a variable is determined by comparing the permuted OOB MSE to unpermuted OOB MSE. Important predictors will
195 result in a large $\%_{\text{incMSE}}$, while a variable of minor importance does little to impact a model's performance, as suggested by a low
196 $\%_{\text{incMSE}}$ value.

197 Partial dependence curves serve as a graphical representation of the relationship between $[\text{NO}_3^-]$ and predictors in the
198 Random Forest model ensemble (Hastie et al., 2009). Each plot considers the effects of other variables in the model, because
199 predictions of $[\text{NO}_3^-]$ are influenced by several predictors when building each tree. In these models, the y-axis of a partial
200 dependence plot represents the average of the OOB predicted $[\text{NO}_3^-]$ at a specific x-value of each predictor.

201 **2.4 Variables and Project Setup**

202 Data from 15 predictors were collected and analysed (Table 1). Spatial variables were manipulated using ArcGIS 10.4.
203 The $[\text{NO}_3^-]$ dataset for the entire NPNRD had 10,676 observations from 1979 to 2014, and was downloaded from the Quality-
204 Assessed Agrichemical Contaminant Database for Nebraska Groundwater (University of Nebraska-Lincoln, 2016). Spatial
205 locations for each well were included in the original $[\text{NO}_3^-]$ dataset and imported into GIS. Wells were clipped to the Dutch Flats
206 model area, resulting in 2,829 $[\text{NO}_3^-]$ observations from 214 wells. In order to have an accurate vadose-zone thickness, only wells
207 with a corresponding depth to groundwater record, of which the most recent record was used, were selected (2,651 observations
208 from 172 wells). Over this period, several wells were sampled much more frequently than others (e.g., monthly sampling, over a
209 short period of record), especially during a U.S. Geological Survey (USGS) National Water-Quality Assessment (NAWQA) study
210 from 1995 to 1999. In order to prevent those wells from dominating the training and testing of the model, annual median $[\text{NO}_3^-]$
211 was calculated for each well and used in the dataset. The dataset was further manipulated such that each median $[\text{NO}_3^-]$ observation
212 had 15 complementary predictors (Table 1). The selected predictor variables capture drivers of long-term $[\text{NO}_3^-]$ and $[\text{NO}_3^-]$ lags.
213 After incorporating all data, including limited records of dissolved oxygen (DO), the final dataset included 1,049 $[\text{NO}_3^-]$
214 observations from 162 wells sampled between 1993 and 2013 (Figure S1A). Additional details of the data selection, sources, and
215 manipulations may be found in the supplemental material.

216 Predictors were divided into two categories: static and dynamic (Table 1). Static predictors are those that either do not
217 change over the period of record, or annual records were limited. DO, for example, could potentially experience slight annual
218 variations, but data were not available to assign each nitrate sample a unique DO value. Instead, observations for each well were
219 assigned the average DO value observed from the well. This approximation was considered reasonable because nitrate isotopic
220 composition and DO data collected in the 1990s and by Wells et al. (2018) did not indicate any major changes to biogeochemical
221 processes over nearly two decades. Total travel time (from ground surface to the point of sampling) was strictly considered a static
222 predictor in this study and was used to link the nitrate-sampling year to a dynamic predictor value.

223 Dynamic predictors were defined in this study as data that changed temporally over the study period. Therefore, each
224 annual median $[\text{NO}_3^-]$ was assigned a lagged dynamic value to represent the difference between the time of a particular surface
225 activity (e.g., timing of a particular irrigation practice) and when groundwater sampling occurred. Dynamic predictors were
226 available from 1946 to 2013 and included annual precipitation, Interstate Canal discharge, area under center pivot sprinklers, and
227 area of planted corn (Fig. 3). Dynamic predictors were included to assess their ability to optimize Random Forest groundwater

228 modelling and determine an appropriate lag time. Lag times were based on the vertical travel distance through both the vadose and
229 saturated zones (see Section 2.5). Area of planted corn was included as a proxy for fertilizer data, which were unavailable prior to
230 1987. However, analysis suggests there has been a 17% reduction (comparing the means of 1987-1999 to 2000-2012) in fertilizer
231 application rates per planted hectare, while area of planted corn has increased 16% (comparing the means of 1983-1999 to 2000-
232 2016) in recent decades (Wells et al., 2018). This trend may be attributed to improved fertilizer management by agricultural
233 producers. There was a likely trade-off in using this proxy; we were able to extend the period of record back to 1946, allowing for
234 analysis of a wider range of lag times in the model, but might have sacrificed some accuracy in recent decades when nitrogen
235 management may have improved. Lastly, vadose and saturated-zone transport rates were assumed to be constant over time (Wells
236 et al., 2018).

237 2.5 Vadose and Saturated-zone Transport Rate Analysis

238 Ranges of vertical velocities (transport rates) through the Dutch Flats vadose zone and saturated zone were estimated
239 from $^3\text{H}/^3\text{He}$ age-dating derived recharge rates. The vertical velocities were determined from results published for samples collected
240 in 1998 (Böhlke et al., 2007, Verstraeten et al., 2001a) and 2016 (Wells et al., 2018) as

$$241 \quad V = \frac{R}{\theta}, \quad (2)$$

242 where R is the upper and lower bound of recharge rates (m/yr), and θ is the mobile water content in the vadose zone or porosity in
243 the saturated zone. The $^3\text{H}/^3\text{He}$ data were used in this study solely for constraining the range of potential transport rates to evaluate
244 in the vadose and saturated zones, and as a base comparison to model results. The age-data, however, were not used by the model
245 itself when seeking to identify an optimum transport rate combination. Throughout the text, unsaturated (vadose)-zone vertical
246 transport rates will be abbreviated as V_u , while saturated-zone vertical transport rates will be V_s . In the vadose zone, θ was assigned
247 a constant value of 0.13, which was calibrated previously using a vertical transport model for the Dutch Flats area (Liao et al.,
248 2012). In the saturated zone, θ was assigned a constant value of 0.35, equal to the value assumed previously for recharge
249 calculations (Böhlke et al., 2007). Vadose and saturated-zone travel times (τ) then were calculated using Equation 3:

$$250 \quad \tau = \frac{z}{V}, \quad (3)$$

251 where τ is either vadose zone (τ_u) or saturated zone (τ_s) travel time in years, and z is the vadose-zone thickness (z_u) or distance
252 from the water table to well mid-screen (z_s) in meters.

253 Though Equations 2 and 3 do not explicitly consider horizontal groundwater flow, they are believed to adequately model
254 shallow groundwater ages, which are likely to follow approximately linear vertical age gradients near the water table. These simple
255 equations are also suggested to sufficiently estimate groundwater age gradients in wedge-shaped aquifers (Cook and Böhlke, 2000),
256 and Böhlke et al. (2007) found a linear model adequately fit their data in the Dutch Flats area. Discrete transport rates and travel
257 times calculated from Equations 2 and 3 should be considered “apparent” rates and travel times, similar to apparent groundwater
258 ages, which are based on imperfect tracers and may be affected by dispersion and mixing. Nonetheless, the saturated open intervals
259 of the monitoring wells used for this study (< 6.1 m for shallow wells; 1.5 m for intermediate and deep wells) generally were short
260 compared with the aquifer thickness, such that age distributions of individual samples were relatively restricted in comparison to
261 those of the whole aquifer or wells with long screened intervals. Additionally, it is emphasized that the assumed mobile water
262 content of 0.13 is a calibrated parameter derived previously through inverse modelling and, as suggested by Liao et al. (2012), may
263 have large uncertainties due to the varying site-specific characteristics known to exist from one well to the next.

264 Because of the influence of canal leakage on both intermediate and deep wells (Böhlke et al., 2007), only recharge rates
265 from shallow wells were used to estimate initial values and permissible ranges of vadose-zone travel times. The mean ($\bar{x} = 0.38$

266 m/yr) and standard deviation ($\sigma = \pm 0.23$ m/yr) of all the 1998 ($n = 7$) and 2016 ($n = 2$) shallow recharge rates were calculated.
267 Using $\bar{x} \pm 1\sigma$, a range of recharge rates from 0.15 to 0.61 m/yr were converted to transport rates (V_u) using Equation 2. One standard
268 deviation was selected to constrain the range of rates evaluated, as we considered this method likely encompassed realistic mean
269 field values. Calculated transport rates resulted in 1.15 to 4.69 m/yr as the range of vadose-zone transport rates. Expanding the
270 upper and lower bounds, a minimum vadose-zone transport rate of 1.0 m/yr and maximum of 4.75 m/yr was applied. Vertical
271 transport rates in the vadose zone were increased by increments of 0.25 m/yr from 1.0 to 4.75 m/yr, resulting in 16 possible vadose-
272 zone transport rates to evaluate in the Random Forest model.

273 Mean ($\bar{x} = 0.84$ m/yr) and standard deviation ($\sigma = \pm 0.73$ m/yr) of all shallow, intermediate, and deep well recharge rates
274 were included in identifying a range of saturated-zone recharge rates from 0.10 to 1.57 m/yr. A total of 35 and 8 recharge rates
275 were used from the Böhlke et al. (2007) and Wells et al. (2018) studies, respectively. Equation 2 was used to calculate saturated-
276 zone transport rates (V_s) of 0.28 and 4.49 m/yr. Saturated-zone transport rates were increased by increments of 0.25 m/yr, from
277 0.25 to 4.5 m/yr, resulting in 18 unique saturated-zone transport rates to evaluate in the Random Forest model. The range of
278 transport rates suggested by groundwater age-dating was large (more than an order of magnitude) and are considered to include
279 rates likely to be expected in a variety of field settings. Presumably, similar model constraints and results could have been obtained
280 without the prior age data and with some relatively conservative estimates.

281 Travel times τ_u and τ_s were calculated for each well based on z_u and z_s , respectively. For every possible combination of
282 vadose and saturated-zone transport rates, a unique total travel time, τ_t , was calculated for each well based on the vadose and
283 saturated-zone dimensions of that particular well.

$$284 \tau_t = \tau_u + \tau_s, \quad (4)$$

285 The total travel times from Equation 4 were used to lag dynamic predictors relative to each nitrate sample date. For
286 instance, a nitrate sample collected in 2010 at a well with a 20-year total travel time (e.g., $\tau_u = 10$ yrs and $\tau_s = 10$ yrs) would be
287 assigned the 1990 values for precipitation (450 mm), Interstate Canal discharge ($0.4 \text{ km}^3/\text{yr}$), center pivot irrigated area (2484
288 hectares), and area of planted corn (8905 hectares).

289 A total of 288 unique transport rate combinations (corresponding to different combinations of the 16 vadose and 18
290 saturated-zone transport rates) were joined into a single dataset totalling over 300,000 observations to determine the optimal rate
291 resulting in the maximum testing NSE from the model. Each transport rate combination incorporated up to 1,049 groundwater
292 $[\text{NO}_3^-]$ values. To decrease runtime, Random Forest models were parallel processed through a Holland Computing Center (HCC)
293 cluster at the University of Nebraska-Lincoln.

294 **3 Results and Discussion**

295 This study addressed a relatively unexplored use of Random Forest, which was to identify optimal lag times based on
296 testing a range of transport rate combinations through the vadose and saturated zones, historical $[\text{NO}_3^-]$, and the use of easily
297 accessible environmental datasets.

298 **3.1. Relative Importance of Transport Time and Dynamic Variables**

299 In our initial modelling with dynamic predictors, we anticipated that we could use the Random Forest model with the
300 highest NSE to identify the optimal pair of vadose and saturated-zone transport rates. However, no clear pattern emerged among
301 the different models (Fig. 4). Given the small differences and lack of defined pattern in testing NSE values, we selected ten transport
302 rate combinations (the five top performing models, plus four transport rate combinations of high and low transport rates, and one

303 intermediate transport rate combination) for further evaluation of variable importance and sensitivity to a range of transport rate
304 combinations (Table 2). Median total travel time ranked third in variable importance, while the four dynamic variables consistently
305 had the four lowest rankings (Fig. 5). Total travel time also had the greatest variability in importance among the fifteen variables,
306 with a range of 18.4% between the upper and lower values, suggesting some model sensitivity to lag times. Excluding total travel
307 time, the remaining variables had an average variable importance range of 6%.

308 Dynamic variables had little influence on the model, despite common potential linkages to groundwater [NO_3^-] (Böhlke
309 et al., 2007; Exner et al., 2010; Spalding et al., 2001). A pattern emerged among dynamic variables where the stronger the historical
310 trend of the predictor, the greater the importance of the predictor (Fig. 3; Fig. 5). For instance, center pivot irrigated area (highest
311 ranking dynamic variable) had the least noise and the most pronounced trend, while annual precipitation (lowest ranking variable)
312 was highly variable and lacked any trend over time (Fig. 3), and also may not be a substantial source of recharge (Böhlke et al.,
313 2007). Further exploration could be done to test more refined variables – for instance, annual median rainfall intensity for the
314 growing season might have a more direct connection to nitrate leaching than total annual precipitation. However, rainfall intensity
315 data are not readily available. Likewise, availability of a long-term, detailed fertilizer loading dataset would be advantageous in
316 providing a more substantiated conclusion regarding the viability of applying dynamic variables to determine vadose and saturated-
317 zone lag. Dynamic variables could be of more use in other study areas that undergo relatively rapid and pronounced changes (e.g.,
318 land use). In future work, the model sensitivity to dynamic variables could be tested through formal sensitivity analysis and/or
319 automated variable selection algorithms (Eibe et al., 2016).

320 Ultimately, results from initial analyses suggest that (1) the dynamic data did little to improve model performance, and
321 (2) Random Forest was not able to relate the four considered dynamic predictors to [NO_3^-] in a meaningful way that could be used
322 to estimate lag time. It is likely the influence of these dynamic predictors is dampened as nitrate is transported from the surface to
323 wells such that data-driven approaches are unable to sort through noise to identify relationships.

324 **3.2 Use of Random Forest to determine transport rates**

325 Due to their low relative importance as predictors, all four dynamic predictors were removed in the subsequent analysis.
326 As discussed above, a notable variation in total travel time %_{inc}MSE was observed in Fig. 5, suggesting model sensitivity to this
327 variable. Additionally, a relationship between travel time and [NO_3^-] has been suggested in the Dutch Flats area through previous
328 studies (Böhlke et al., 2007; Wells et al., 2018). Therefore, a second analysis of just the 11 static predictors was performed over
329 the full range of vadose and saturated transport rates (i.e., 288 combinations). However, in the second analysis, model sensitivity
330 to total travel time – evaluated with respect to the transport rate combination corresponding to the largest %_{inc}MSE of total travel
331 time – was used to determine a distinguished transport rate combination. In other words, models were re-trained and tested for all
332 transport rate combinations, each of which produced a unique set of values for the total travel time variable. As described in Section
333 2.3, the %_{inc}MSE value for total travel time was then based on the error induced in the model by permuting the calculated total
334 travel times across all the nitrate observations (i.e., randomly shuffling the total travel time variable, and thus disturbing the
335 structure of the dataset).

336 The Random Forest models were useful in identifying the relative magnitudes of V_u and V_s that led to high %_{inc}MSE.
337 Based on the heat map of %_{inc}MSE, a band of transport rate combinations with consistently high %_{inc}MSE was visually apparent
338 (Fig. 6). The upper and lower bounds of the band translate to transport rate ratios (V_s/V_u) ranging from 0.9 to 1.5, and are values
339 that could be useful in constraining recharge and/or transport rate estimates in more complex mechanistic models, as part of a
340 hybrid modelling approach. This is especially important because recharge is one of the most sensitive parameters in a groundwater
341 model (Mittelstet et al., 2011), yet one with high uncertainty. Whereas a saturated-zone velocity that is greater than a vadose-zone

342 velocity would be unexpected in many unconsolidated surficial aquifers receiving distributed recharge, the statistical machine
343 learning results are consistent with two contrasting primary recharge processes in the Dutch Flats area: (1) diffuse recharge from
344 irrigation and precipitation across the landscape, and (2) focused recharge from leaking irrigation conveyance canals.

345 The %_{inc}MSE of total travel time in the second analysis ranged from 20.6 to 31.5%, with the largest %_{inc}MSE associated
346 with vadose and saturated-zone transport rates of 3.50 m/yr and 3.75 m/yr, respectively (Fig. 6), and the top four predictors for this
347 transport rate combination were total travel time, vadose-zone thickness, dissolved oxygen, and saturated thickness (Fig. 7).
348 Converting those vadose and saturated-zone transport rates to recharge rates yielded values of 0.46 m/yr and 1.31 m/yr,
349 respectively. Such a large difference between the two recharge values is consistent with the hydrologic conceptual model of the
350 Dutch Flats area. In fact, both model recharge rates compare favourably with recharge rates calculated from the previous Dutch
351 Flats studies using ³H/³He age-dating (Böhlke et al., 2007; Wells et al., 2018). For instance, the recharge rate determined from the
352 vadose-zone transport rate in this study (0.46 m/yr) was comparable to the mean recharge rate of 0.38 m/yr (n = 9) from
353 groundwater age-dating at shallow wells, which are most representative of diffuse recharge below crop fields that are present across
354 most of the study area (e.g., Figure S2). Additionally, the recharge rate (1.31 m/yr) determined from the saturated-zone transport
355 rate was consistent with the mean recharge value derived from groundwater ages in intermediate wells (1.22 m/yr, n = 13).
356 Intermediate wells are variably impacted by focused recharge from canals in upgradient areas. Given the similarity in diffuse
357 recharge and focused recharge estimates from both Random Forest and groundwater age-dating, the transport rate ratios (1.2 and
358 1.1, respectively) were consistent. That is, the Random Forest modelling framework produced transport rates consistent with the
359 major hydrological processes in Dutch Flats both in direct (i.e., transport rate estimates) and relative (i.e., transport rate ratio)
360 terms.

361 Assuming the Random Forest approach has accurately captured the two major recharge processes (diffuse recharge over
362 crop fields and focused recharge from canals), a comparison of recharge rates from all sampled groundwater wells representative
363 of recharge to the groundwater system as a whole (0.84 m/yr, n = 43) to the recharge rates from Random Forest modelling (0.46
364 and 1.31 m/yr) would provide an estimate of the relative importance of diffuse versus focused recharge on overall recharge in
365 Dutch Flats. Under these assumptions, diffuse recharge would account for approximately 55%, while focused recharge would
366 account for about 45% of total recharge in the Dutch Flats area. Similarly, Böhlke et al. (2007) concluded that these two recharge
367 sources contributed roughly equally to the aquifer on the basis of groundwater age profiles, as well as from dissolved atmospheric
368 gas data indicating mean recharge temperatures between those expected of diffuse infiltration and focused canal leakage.

369 Partial dependence plots, which illustrate the impact a single predictor has on [NO₃⁻] in the model with respect to other
370 predictors (Fig. 8), largely reflect the conceptual understanding of the system from previous studies including Böhlke et al. (2007)
371 and Wells et al. (2018). Key features that strengthen confidence in the Random Forest modelling include (1) depth to bottom
372 screen, where groundwater [NO₃⁻] is lower at greater depths, (2) the effects of minor and major canals, where groundwater [NO₃⁻]
373 in the vicinity of canals is diluted by canal leakage, and the influence of major canals extends a longer distance when compared to
374 that of minor canals, (3) land surface elevation, where elevations indicating proximity to major canals are associated with relatively
375 lower groundwater [NO₃⁻], and (4) DO concentration, where higher DO concentration is linked to higher groundwater [NO₃⁻]. We
376 note that decreasing DO and [NO₃⁻] with groundwater age can be explained by DO reduction and historical changes in [NO₃⁻]
377 recharge, whereas groundwater chemistry and nitrate isotopic data recorded in both this study and previous Dutch Flats studies
378 suggest denitrification was not a major factor in this alluvial aquifer.

379 The partial dependence plot (Fig. 8) for total travel time exhibits a pronounced threshold, where [NO₃⁻] is markedly higher
380 for groundwater with travel time less than seven years. It is possible this reflects long-term stratification of groundwater [NO₃⁻],
381 stemming from the suggested patterns stated above as nitrate varies with aquifer depth due to the influences of diffuse and focused

382 recharge in the region. This seven-year threshold is slightly lower than a previous estimate of mean groundwater age in the aquifer
383 (8.8 years; Böhlke et al., 2007; where groundwater age excludes vadose-zone travel time) and suggests that shallow groundwater
384 can respond relatively rapidly to changes in nitrogen management in the Dutch Flats area.

385 **3.3 Opportunities and limitations of Random Forest approach in estimating lag times**

386 Overall, results suggest that in a complex system such as Dutch Flats, Random Forest was able to identify reasonable
387 transport rates for both the vadose and saturated zones, and with additional validation, this method may offer an inexpensive (i.e.,
388 compared to groundwater age-dating across a large monitoring well network and/or complex modelling) and reasonable technique
389 for estimating lag time from historical monitoring data. Further, this approach allows for additional insight on groundwater
390 dynamics to be extracted from existing monitoring data. However, this study was conducted in the context of a larger project
391 (Wells et al., 2018) and built on prior research on groundwater flow and $[\text{NO}_3^-]$ in the study area (Böhlke et al., 2007). Therefore,
392 it is critical in future work to incorporate site-specific knowledge, process understanding, and approaches for increasing
393 interpretability of machine learning models (Lundberg et al., 2020, Saia et al., 2020), as highlighted in key considerations below.

394

395 Some key considerations for future application of this approach include:

- 396 (1) The Random Forest approach might be useful for estimating future recharge and $[\text{NO}_3^-]$ using multiple potential
397 management scenarios, as long as considered management scenarios fall within the range of historical observations used
398 to train the model. This information could be used to inform policy makers of the impact that current and future
399 management decisions will have on recharge and $[\text{NO}_3^-]$.
- 400 (2) The Dutch Flats overlies a predominantly oxic aquifer, where nitrate transport is mostly conservative. In aquifers with
401 both oxic and anoxic conditions and distinct nitrate extinction depths (Liao et al., 2012; Welch et al., 2011), this approach
402 may be biased toward oxic portions of the aquifer where the nitrate signal is preserved. Similarly, vertical profiles of
403 $[\text{NO}_3^-]$ and isotopic composition in the vadose zone could provide valuable data to investigate (1) the amount of nitrate
404 stored in the vadose zone, and (2) whether nitrate undergoes any biogeochemical changes while being transported through
405 the vadose zone to the water table.
- 406 (3) While estimates of vadose and saturated-zone transport rates determined from $\%_{\text{inc}}\text{MSE}$ are consistent with previous
407 studies, the predictive performance of the selected model (based on NSE and visual inspection of predicted versus
408 observed nitrate plots) was not substantially different than other models tested. In other words, the “optimal model” was
409 only weakly preferred in terms of predicting $[\text{NO}_3^-]$. Testing the approach of using $\%_{\text{inc}}\text{MSE}$ in other vadose and saturated
410 zones, with substantial comparison to previous transport rate estimates, is warranted. This would be especially valuable
411 in an area with a well-defined input function for nitrate that could be compared to a reconstructed input function from the
412 model. Further, in aquifer settings with relatively evenly distributed recharge, optimized travel times to wells could be
413 used to estimate the infiltration date of samples, thus providing an optimized view of historical variation of $[\text{NO}_3^-]$ entering
414 the subsurface, as illustrated in Figure S1B. In the Dutch Flats area, however, such an analysis is complicated by effects
415 of subsurface nitrate dilution by local recharge from canal leakage.
- 416 (4) Despite potential non-uniqueness in prediction metrics, the heat map of $\%_{\text{inc}}\text{MSE}$ did reveal an orderly pattern suggesting
417 consistent transport rate ratios. For modelling efforts where recharge rates are a key calibration parameter, identification
418 of a range of reasonable recharge rates, and/or the ratio of recharge rates from diffuse and focused recharge sources for a
419 complex system will reduce model uncertainty and improve results. This statistical machine learning approach, which
420 essentially leverages nitrate as a tracer (albeit with an unknown input function in this case), may provide valuable insight

421 to complement relatively expensive groundwater age-dating or vadose-zone monitoring data, or as a standalone approach
422 for first-order approximations.

423 (5) The demonstrated statistical machine learning approach is apparently well-suited for drawing out transport rate
424 information from a site with two distinct recharge sources (diffuse versus focused recharge sources) driving the
425 groundwater nitrate dynamics. Further testing is needed at sites where recharge and nitrate dynamics are more subtle.

426 **4 Conclusions**

427 The Dutch Flats area exhibits large variations in $[\text{NO}_3^-]$ throughout a relatively small region in western Nebraska. Long-
428 term groundwater $[\text{NO}_3^-]$ monitoring and previous groundwater age-dating studies in Dutch Flats provided an opportune setting to
429 test a new application of statistical machine learning (Random Forest) for determining vadose and saturated-zone transport rates.
430 Overall results suggest Random Forest has the capability to both identify reasonable transport rates (and lag time) and key variables
431 influencing groundwater $[\text{NO}_3^-]$, albeit with potential for non-unique results. Limitations were also identified when using dynamic
432 predictors to model groundwater $[\text{NO}_3^-]$. Utilizing only static predictors, and Random Forest's ability to evaluate variable
433 importance, vadose-zone and saturated-zone transport rates were selected based on model sensitivity to changing the total travel
434 time predictor. In other words, total travel time variable importance was evaluated for 288 different transport rate combinations,
435 and the combination with a total travel time having the largest influence over the model's ability to predict $[\text{NO}_3^-]$ was selected for
436 additional examination. This analysis identified a vadose-zone and saturated-zone transport rate combination consistent with rates
437 previously estimated from $^3\text{H}/^3\text{He}$ age-dating in Böhlke et al. (2007) and Wells et al. (2018), indicating a combination of distributed
438 and focused sources of irrigation recharge to this aquifer

439 Future studies should include assessments of the proper conditions for application of dynamic predictors and include
440 comparisons of data-driven analyses with complementary datasets. Despite noted limitations, partial dependence plots and relative
441 importance of predictors were largely consistent with previous findings and mechanistic understanding of the study area, giving
442 greater confidence in model outputs. The influence of canal leakage on groundwater recharge rates and $[\text{NO}_3^-]$, for example, was
443 consistent with previous Dutch Flats studies. Partial dependence plots suggest a threshold of higher $[\text{NO}_3^-]$ for groundwater with
444 total travel time (vadose and saturated-zone travel times, combined) of less than seven years, indicating the potential for relatively
445 rapid groundwater $[\text{NO}_3^-]$ response to widespread implementation of best management practices. Additionally, research is needed
446 to determine the minimum number of observations needed to effectively apply the framework shown here.

447

448 **Author contribution:** TG, AM, and NN were responsible for conceptualization. MW and NN developed the model code and MW
449 performed formal analysis. MW prepared the manuscript from his M.S. thesis with contributions from all co-authors, including
450 JKB. TG was responsible for project administration and funding acquisition.

451

452 **Acknowledgements:** The authors acknowledge the North Platte Natural Resources District for providing technical assistance and
453 resources, including long-term groundwater nitrate data accessed via the Quality-Assessed Agrichemical Contaminant Database
454 for Nebraska Groundwater. We thank Steve Sibray and Mason Johnson for their support in field sampling efforts and Les Howard
455 for cartography. We also thank Christopher Green, Sophie Ehrhardt, Scott Gardner, and an anonymous reviewer for helpful
456 comments on earlier versions of the paper. Any use of trade, firm, or product names is for descriptive purposes only and does not
457 imply endorsement by the U.S. Government.

458

460 **Funding:** This work was supported by the U.S. Geological Survey 104b Program (Project 2016NE286B), U.S. Department of
461 Agriculture—National Institute of Food and Agriculture NEB-21-177 (Hatch Project 1015698), and Daugherty Water for Food
462 Global Institute Graduate Student Fellowship.

463

464 **Code and Data Availability:** Code is available on request. Data used in the random forest model and described in the supplemental
465 information is available via the University of Nebraska – Lincoln Data Repository (<https://doi.org/10.32873/unl.dr.20200428>).

466 References

467 Anning, D. W., Paul, A. P., McKinney, T. S., Huntington, J. M., Bexfield, L. M. and Thiros, S. A.: Predicted nitrate and arsenic
468 concentrations in basin-fill aquifers of the Southwestern United States, Report, United States Geological Survey. [online] Available
469 from: <https://pubs.usgs.gov/sir/2012/5065/>, 2012.

470 Babcock, H. M., Visher, F. N. and Durum, W. H.: Ground-water conditions in the Dutch Flats area, Scotts Bluff and Sioux
471 Counties, Nebraska, with a section on chemical quality of the ground water, Report. [online] Available from:
472 <http://pubs.er.usgs.gov/publication/cir126>, 1951.

473 Ball, L. B., Kress, W. H., Steele, G. V., Cannia, J. C. and Andersen, M. J.: Determination of canal leakage potential using
474 continuous resistivity profiling techniques, Interstate and Tri-State Canals, western Nebraska and eastern Wyoming, 2004, Report,
475 United States Geological Survey. [online] Available from: <http://pubs.er.usgs.gov/publication/sir20065032>, 2006.

476 Böhlke, J. K.: Groundwater recharge and agricultural contamination, *Hydrogeology Journal*, 10(1), 153–179, doi:10.1007/s10040-
477 001-0183-3, 2002.

478 Böhlke, J. K. and Denver, J. M.: Combined Use of Groundwater Dating, Chemical, and Isotopic Analyses to Resolve the History
479 and Fate of Nitrate Contamination in Two Agricultural Watersheds, Atlantic Coastal Plain, Maryland, *Water Resources Research*,
480 31(9), 2319–2339, doi:10.1029/95WR01584, 1995.

481 Böhlke, J. K., Wanty, R., Tuttle, M., Delin, G. and Landon, M.: Denitrification in the recharge area and discharge area of a transient
482 agricultural nitrate plume in a glacial outwash sand aquifer, Minnesota: Denitrification in recharge and discharge areas, *Water
483 Resources Research*, 38(7), 10-1-10–26, doi:10.1029/2001WR000663, 2002.

484 Böhlke, J. K., Verstraeten, I. M. and Kraemer, T. F.: Effects of surface-water irrigation on sources, fluxes, and residence times of
485 water, nitrate, and uranium in an alluvial aquifer, *Applied Geochemistry*, 22(1), 152–174, doi:10.1016/j.apgeochem.2006.08.019,
486 2007.

487 Breiman, L.: *Random Forests*, *Machine Learning*, 45(1), 5–32, doi:10.1023/A:1010933404324, 2001.

488 Browne, B. A. and Guldan, N. M.: Understanding Long-Term Baseflow Water Quality Trends Using a Synoptic Survey of the
489 Ground Water–Surface Water Interface, Central Wisconsin, *Journal of Environment Quality*, 34(3), 825,
490 doi:10.2134/jeq2004.0134, 2005.

491 Cherry, M., Gilmore, T., Mittelstet, A., Gastmans, D., Santos, V. and Gates, J. B.: Recharge seasonality based on stable isotopes:
492 Nongrowing season bias altered by irrigation in Nebraska, *Hydrological Processes*, doi:10.1002/hyp.13683, 2020.

493 Cook, P. G. and Böhlke, J. K.: Determining Timescales for Groundwater Flow and Solute Transport, in *Environmental Tracers in
494 Subsurface Hydrology*, edited by P. G. Cook and A. L. Herczeg, pp. 1–30, Springer US, Boston, MA., 2000.

495 Dieter, C. A., Maupin, M. A., Caldwell, R. R., Harris, M. A., Ivahnenko, T. I., Lovelace, J. K., Barber, N. L. and Linsey, K. S.:
496 Estimated use of water in the United States in 2015, Report, Reston, VA., 2018.

497 Eberts, S. M., Thomas, M. S. and Jagucki, M. L.: The quality of our Nation’s waters—Factors affecting public-supply-well
498 vulnerability to contamination—Understanding observed water quality and anticipating future water quality, U.S. Geological
499 Survey Circular 1385. [online] Available from: <https://pubs.usgs.gov/circ/1385/>, 2013.

- 500 Efron, B.: Bootstrap Methods: Another Look at the Jackknife, *The Annals of Statistics*, 7(1), 1–26, doi:10.1214/aos/1176344552,
501 1979.
- 502 Eibe, F., Hall, M. A. and Witten, I. H.: The WEKA Workbench, in Online Appendix for “Data Mining: Practical Machine Learning
503 Tools and Techniques,” Morgan Kaufmann., 2016.
- 504 Exner, M. E., Perea-Estrada, H. and Spalding, R. F.: Long-Term Response of Groundwater Nitrate Concentrations to Management
505 Regulations in Nebraska’s Central Platte Valley, *The Scientific World Journal*, 10, 286–297, doi:10.1100/tsw.2010.25, 2010.
- 506 Gilmore, T. E., Genereux, D. P., Solomon, D. K. and Solder, J. E.: Groundwater transit time distribution and mean from streambed
507 sampling in an agricultural coastal plain watershed, North Carolina, USA: Groundwater transit time, *Water Resources Research*,
508 52(3), 2025–2044, doi:10.1002/2015WR017600, 2016.
- 509 Green, C. T., Liao, L., Nolan, B. T., Juckem, P. F., Shope, C. L., Tesoriero, A. J. and Jurgens, B. C.: Regional Variability of Nitrate
510 Fluxes in the Unsaturated Zone and Groundwater, Wisconsin, USA, *Water Resources Research*, 54(1), 301–322,
511 doi:10.1002/2017WR022012, 2018.
- 512 Harvey, F. E. and Sibray, S. S.: Delineating Ground Water Recharge from Leaking Irrigation Canals Using Water Chemistry and
513 Isotopes, *Ground Water*, 39(3), 408–421, doi:10.1111/j.1745-6584.2001.tb02325.x, 2001.
- 514 Hastie, T., Tibshirani, R. and Friedman, J. H.: *The elements of statistical learning: data mining, inference, and prediction*, 2nd ed.,
515 Springer, New York, NY., 2009.
- 516 Hobza, C. M. and Andersen, M. J.: Quantifying canal leakage rates using a mass-balance approach and heat-based hydraulic
517 conductivity estimates in selected irrigation canals, western Nebraska, 2007 through 2009, Report, United States Geological
518 Survey. [online] Available from: <http://pubs.er.usgs.gov/publication/sir20105226>, 2010.
- 519 Homer, C. G., Dewitz, J., Yang, L., Jin, S., Danielson, P., Xian, G. Z., Coulston, J., Herold, N., Wickham, J. and Megown, K.:
520 Completion of the 2011 National Land Cover Database for the conterminous United States – Representing a decade of land cover
521 change information, *Photogrammetric Engineering and Remote Sensing*, 81, 345354, 2015.
- 522 Hudson, C. (NPNRD): Personal Communication with M.J. Wells, University of Nebraska, Lincoln, NE, USA, 2018.
- 523 Ilampooranan, I., Van Meter, K. J. and Basu, N. B.: A Race against Time: Modelling Time Lags in Watershed Response, *Water
524 Resources Research*, doi:10.1029/2018WR023815, 2019.
- 525 Irmak, S., Odhiambo, L., Kranz, W. L. and Eisenhauer, D. E.: Irrigation Efficiency And Uniformity, And Crop Water Use
526 Efficiency, Extension Circular, University of Nebraska – Lincoln, Lincoln, NE. [online] Available from: Available at
527 <http://extensionpubs.unl.edu/>, 2011.
- 528 Jones, Z. M. and Linder, F. J.: Exploratory Data Analysis using Random Forests, in 73rd Annual MPSA Conference, pp. 1–31.
529 [online] Available from: http://zmjones.com/static/papers/rfss_manuscript.pdf (Accessed 25 May 2018), 2015.
- 530 Juntakut, P., Snow, D. D., Haacker, E. M. K. and Ray, C.: The long term effect of agricultural, vadose zone and climatic factors
531 on nitrate contamination in Nebraska’s groundwater system, *Journal of Contaminant Hydrology*, 220, 33–48,
532 doi:10.1016/j.jconhyd.2018.11.007, 2019.
533
- 534 Kennedy, C. D., Genereux, D. P., Corbett, D. R. and Mitasova, H.: Spatial and temporal dynamics of coupled groundwater and
535 nitrogen fluxes through a streambed in an agricultural watershed: Groundwater and nitrogen fluxes in a streambed, *Water
536 Resources Research*, 45(9), doi:10.1029/2008WR007397, 2009.
- 537 Knoll, L., Breuer, L. and Bach, M.: Nation-wide estimation of groundwater redox conditions and nitrate concentrations through
538 machine learning, *Environmental Research Letters*, 15(6), 064004, doi:10.1088/1748-9326/ab7d5c, 2020.
539
- 540 Kuhn, M.: Building Predictive Models in *R* Using the caret Package, *Journal of Statistical Software*, 28(5),
541 doi:10.18637/jss.v028.i05, 2008.
- 542 Liao, L., Green, C. T., Bekins, B. A. and Böhlke, J. K.: Factors controlling nitrate fluxes in groundwater in agricultural areas:
543 Factors controlling nitrate fluxes in groundwater, *Water Resources Research*, 48(6), doi:10.1029/2011WR011008, 2012.

- 544 Luckey, R. R. and Cannia, J. C.: Groundwater Flow Model of the Western Model Unit of the Nebraska Cooperative Hydrology
545 Study (COHYST) Area, Nebraska Department of Natural Resources, Lincoln, NE. [online] Available from:
546 ftp://ftp.dnr.nebraska.gov/Pub/cohystrftp/cohystr/model_reports/WMU_Documentation_060519.pdf, 2006.
- 547 Lundberg, S. M., Erion, G., Chen, H., DeGrave, A., Prutkin, J. M., Nair, B., Katz, R., Himmelfarb, J., Bansal, N. and Lee, S.-I.:
548 From local explanations to global understanding with explainable AI for trees, *Nature Machine Intelligence*, 2(1), 56–67,
549 doi:10.1038/s42256-019-0138-9, 2020.
- 550
551 McMahon, P. B., Dennehy, K. F., Bruce, B. W., Böhlke, J. K., Michel, R. L., Gurdak, J. J. and Hurlbut, D. B.: Storage and transit
552 time of chemicals in thick unsaturated zones under rangeland and irrigated cropland, High Plains, United States: Chemical storage
553 in thick unsaturated zone, *Water Resources Research*, 42(3), doi:10.1029/2005WR004417, 2006.
- 554 Meals, D. W., Dressing, S. A. and Davenport, T. E.: Lag Time in Water Quality Response to Best Management Practices: A
555 Review, *Journal of Environment Quality*, 39(1), 85, doi:10.2134/jeq2009.0108, 2010.
- 556 Mittelstet, A. R., Smolen, M. D., Fox, G. A. and Adams, D. C.: Comparison of Aquifer Sustainability Under Groundwater
557 Administrations in Oklahoma and Texas: Comparison of Aquifer Sustainability Under Groundwater Administrations in Oklahoma
558 and Texas, *JAWRA Journal of the American Water Resources Association*, 47(2), 424–431, doi:10.1111/j.1752-
559 1688.2011.00524.x, 2011.
- 560 Morgenstern, U., Daughney, C. J., Leonard, G., Gordon, D., Donath, F. M. and Reeves, R.: Using groundwater age and
561 hydrochemistry to understand sources and dynamics of nutrient contamination through the catchment into Lake Rotorua, New
562 Zealand, *Hydrology and Earth System Sciences*, 19(2), 803–822, doi:10.5194/hess-19-803-2015, 2015.
- 563 Nash, J. E. and Sutcliffe, J. V.: River flow forecasting through conceptual models part I — A discussion of principles, *Journal of*
564 *Hydrology*, 10(3), 282–290, doi:10.1016/0022-1694(70)90255-6, 1970.
- 565 NASS: USDA/NASS QuickStats Ad-hoc Query Tool, [online] Available from: <https://quickstats.nass.usda.gov/> (Accessed 15
566 February 2018), 2018.
- 567 NEDNR: Fifty-fifth biennial report of the Department of Natural Resources, Nebraska Department of Natural Resources, Lincoln,
568 NE. [online] Available from: [https://dnr.nebraska.gov/sites/dnr.nebraska.gov/files/doc/surface-water/biennial-](https://dnr.nebraska.gov/sites/dnr.nebraska.gov/files/doc/surface-water/biennial-reports/BiennialReport2005-06.pdf)
569 [reports/BiennialReport2005-06.pdf](https://dnr.nebraska.gov/sites/dnr.nebraska.gov/files/doc/surface-water/biennial-reports/BiennialReport2005-06.pdf), 2009.
- 570 Nelson, N. G., Muñoz-Carpena, R., Phlips, E. J., Kaplan, D., Sucsy, P. and Hendrickson, J.: Revealing Biotic and Abiotic Controls
571 of Harmful Algal Blooms in a Shallow Subtropical Lake through Statistical Machine Learning, *Environmental Science &*
572 *Technology*, 52(6), 3527–3535, doi:10.1021/acs.est.7b05884, 2018.
- 573 NOAA: National Climatic Data Center (NCDC), [online] Available from: <https://www.ncdc.noaa.gov/cdo-web/datatools>
574 (Accessed 4 August 2017), 2017.
- 575 Nolan, B. T., Green, C. T., Juckem, P. F., Liao, L. and Reddy, J. E.: Metamodeling and mapping of nitrate flux in the unsaturated
576 zone and groundwater, Wisconsin, USA, *Journal of Hydrology*, 559, 428–441, doi:10.1016/j.jhydrol.2018.02.029, 2018.
- 577 Nolan, B. T., Gronberg, J. M., Faunt, C. C., Eberts, S. M. and Belitz, K.: Modeling Nitrate at Domestic and Public-Supply Well
578 Depths in the Central Valley, California, *Environmental Science & Technology*, 48(10), 5643–5651, doi:10.1021/es405452q,
579 2014.
- 580 NRCS: Web Soil Survey. [online] Available from: <https://websoilsurvey.sc.egov.usda.gov/> (Accessed 16 November 2017), 2018.
- 581 Ouedraogo, I., Defourny, P. and Vanclooster, M.: Validating a continental-scale groundwater diffuse pollution model using
582 regional datasets, *Environmental Science and Pollution Research*, doi:10.1007/s11356-017-0899-9, 2017.
- 583 Preston, T. (NPNRD): Personal Communication with M.J. Wells, University of Nebraska, Lincoln, NE, USA, 2017.
- 584 Puckett, L. J., Tesoriero, A. J. and Dubrovsky, N. M.: Nitrogen Contamination of Surficial Aquifers—A Growing Legacy †,
585 *Environmental Science & Technology*, 45(3), 839–844, doi:10.1021/es1038358, 2011.

586 R Core Team: R: A language and environment for statistical computing, R Foundation for Statistical Computing, Vienna, Austria.
587 [online] Available from: <https://www.R-project.org/>, 2017.

588 Rahmati, O., Choubin, B., Fathabadi, A., Coulon, F., Soltani, E., Shahabi, H., Mollaeafar, E., Tiefenbacher, J., Cipullo, S., Ahmad,
589 B. B. and Tien Bui, D.: Predicting uncertainty of machine learning models for modelling nitrate pollution of groundwater using
590 quantile regression and UNEEC methods, *Science of The Total Environment*, 688, 855–866, doi:10.1016/j.scitotenv.2019.06.320,
591 2019.

592

593 Ransom, K. M., Nolan, B. T., A. Traum, J., Faunt, C. C., Bell, A. M., Gronberg, J. A. M., Wheeler, D. C., Z. Rosecrans, C.,
594 Jurgens, B., Schwarz, G. E., Belitz, K., M. Eberts, S., Kourakos, G. and Harter, T.: A hybrid machine learning model to predict
595 and visualize nitrate concentration throughout the Central Valley aquifer, California, USA, *Science of The Total Environment*,
596 601–602, 1160–1172, doi:10.1016/j.scitotenv.2017.05.192, 2017.

597 Rodriguez-Galiano, V. F., Mendes, M. P., Garcia-Soldado, M. J., Chica-Olmo, M. and Ribeiro, L.: Predictive modeling of
598 groundwater nitrate pollution using Random Forest and multisource variables related to intrinsic and specific vulnerability: A case
599 study in an agricultural setting (Southern Spain), *Science of The Total Environment*, 476–477, 189–206,
600 doi:10.1016/j.scitotenv.2014.01.001, 2014.

601 Rossman, N. R., Zlotnik, V. A., Rowe, C. M. and Szilagyi, J.: Vadose zone lag time and potential 21st century climate change
602 effects on spatially distributed groundwater recharge in the semi-arid Nebraska Sand Hills, *Journal of Hydrology*, 519, 656–669,
603 doi:10.1016/j.jhydrol.2014.07.057, 2014.

604 Russoniello, C. J., Konikow, L. F., Kroeger, K. D., Fernandez, C., Andres, A. S. and Michael, H. A.: Hydrogeologic controls on
605 groundwater discharge and nitrogen loads in a coastal watershed, *Journal of Hydrology*, 538, 783–793,
606 doi:10.1016/j.jhydrol.2016.05.013, 2016.

607 Saia, S. M., Nelson, N., Huseth, A. S., Grieger, K. and Reich, B. J.: Transitioning Machine Learning from Theory to Practice in
608 Natural Resources Management, *Ecological Modelling*, 435, 109257, doi:10.1016/j.ecolmodel.2020.109257, 2020.

609

610 Spalding, R. F., Watts, D. G., Schepers, J. S., Burbach, M. E., Exner, M. E., Poreda, R. J. and Martin, G. E.: Controlling Nitrate
611 Leaching in Irrigated Agriculture, *Journal of Environment Quality*, 30(4), 1184, doi:10.2134/jeq2001.3041184x, 2001.

612 Turkeltaub, T., Kurtzman, D. and Dahan, O.: Real-time monitoring of nitrate transport in the deep vadose zone under a crop field
613 – implications for groundwater protection, *Hydrology and Earth System Sciences*, 20(8), 3099–3108, doi:10.5194/hess-20-3099-
614 2016, 2016.

615 University of Nebraska-Lincoln (UNL): Quality-Assessed Agrichemical Contaminant Database for Nebraska Ground Water,
616 [online] Available from: <https://clearinghouse.nebraska.gov/Clearinghouse.aspx> (Accessed 5 September 2016), 2016.

617 USBR: Hydromet: Archive Data Access, [online] Available from: https://www.usbr.gov/gp/hydromet/hydromet_arcread.html
618 (Accessed 22 May 2018), 2018.

619 USDA: NAIP and NAPP Imagery, [online] Available from <https://dnr.nebraska.gov/data/digital-imagery> (Accessed 14 August
620 2017), 2017

621 U.S. Geological Survey [USGS]: National Elevation Dataset (NED), [online] Available from: <https://datagateway.nrcs.usda.gov/>
622 (Accessed 08 October 2020), 1997.

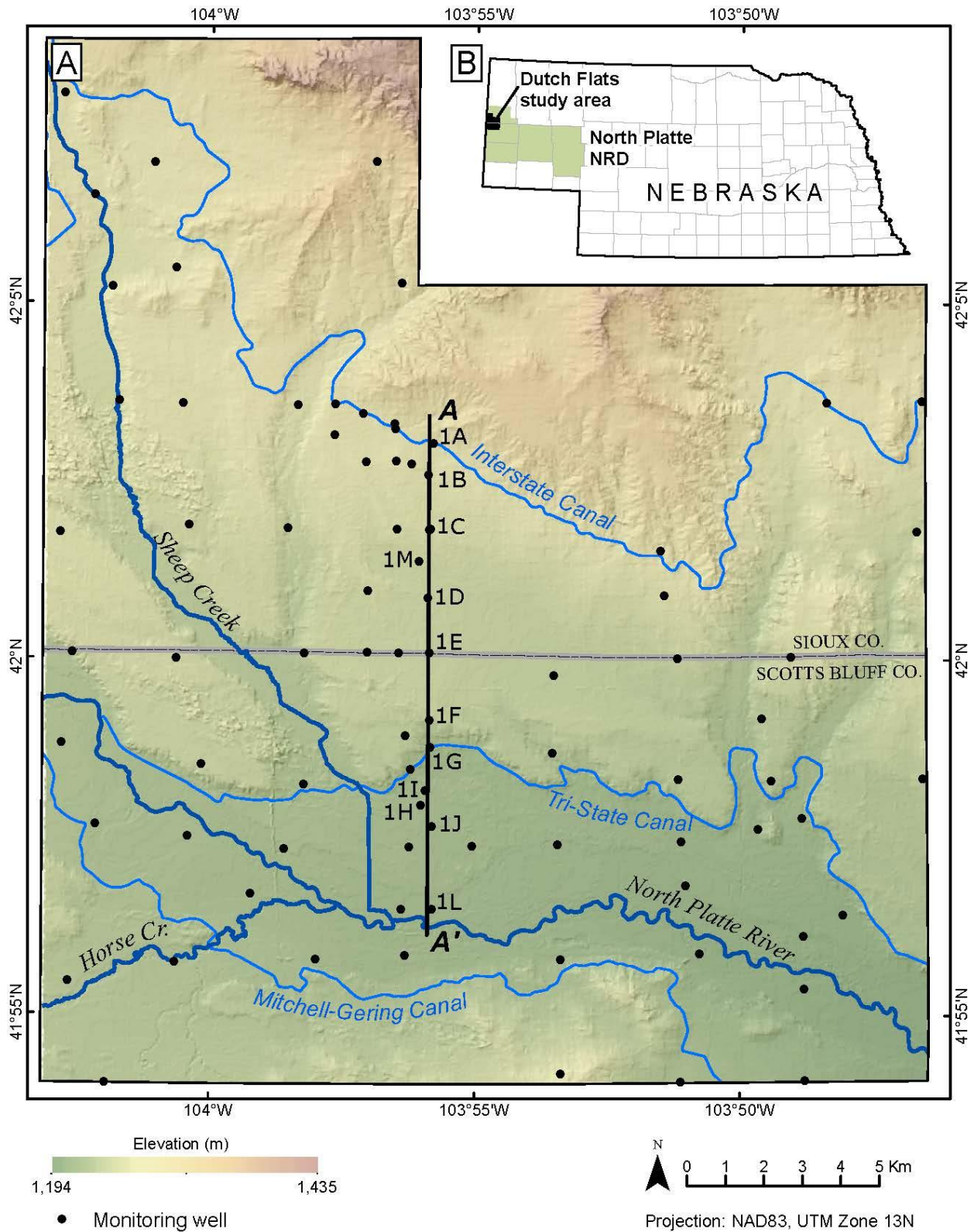
623 U.S. Geological Survey [USGS]: LANDSAT Imagery, [online] Available from: <https://earthexplorer.usgs.gov/> (Accessed 14
624 August 2017), 2017.

625 U.S. Geological Survey [USGS]: NHDPlus High Resolution, [online] Available from: https://nhd.usgs.gov/NHDPlus_HR.html
626 (Accessed 29 June 2018), 2012.

627 Van Meter, K. J. and Basu, N. B.: Catchment Legacies and Time Lags: A Parsimonious Watershed Model to Predict the Effects
628 of Legacy Storage on Nitrogen Export, edited by Y. Hong, *PLoS ONE*, 10(5), e0125971, doi:10.1371/journal.pone.0125971, 2015.

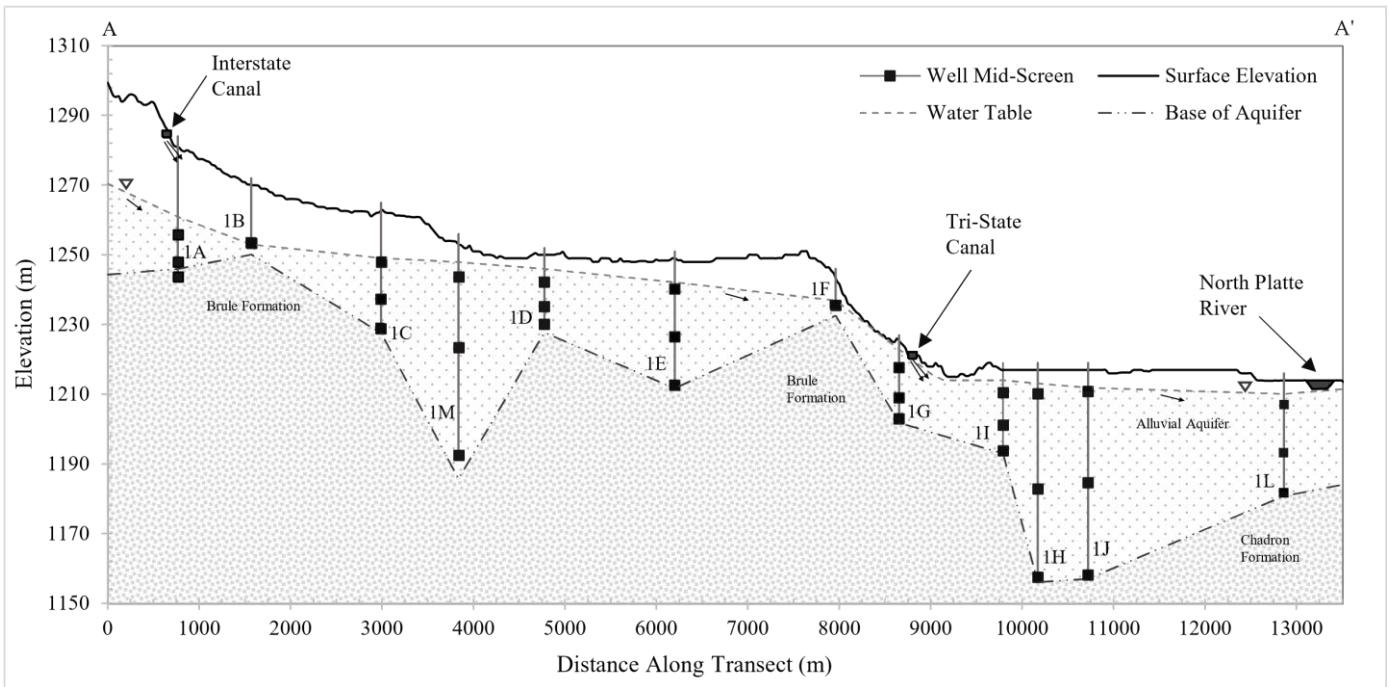
629 Van Meter, K. J. and Basu, N. B.: Time lags in watershed-scale nutrient transport: an exploration of dominant controls,
630 *Environmental Research Letters*, 12(8), 084017, doi:10.1088/1748-9326/aa7bf4, 2017.

- 631 Vanclooster, M., Petit, S., Bogaert, P. and Lietar, A.: Modelling Nitrate Pollution Vulnerability in the Brussel's Capital Region
632 (Belgium) Using Data-Driven Modelling Approaches, *Journal of Water Resource and Protection*, 12(05), 416–430,
633 doi:10.4236/jwarp.2020.125025, 2020.
- 634
- 635 Verstraeten, I. M., Sibray, S. S., Cannia, J. C. and Tanner, D. Q.: Reconnaissance of ground-water quality in the North Platte
636 Natural Resources District, western Nebraska, June-July 1991, Report, United States Geological Survey. [online] Available from:
637 <http://pubs.er.usgs.gov/publication/wri944057>, 1995.
- 638 Verstraeten, I. M., Steele, G. V., Cannia, J. C., Böhlke, J. K., Kraemer, T. E., Hitch, D. E., Wilson, K. E. and Carnes, A. E.: Selected
639 field and analytical methods and analytical results in the Dutch Flats area, western Nebraska, 1995-99, Report, United States
640 Geological Survey, Reston, VA. [online] Available from: <http://pubs.er.usgs.gov/publication/ofr00413>, 2001 a.
- 641 Verstraeten, I. M., Steele, G. V., Cannia, J. C., Hitch, D. E., Scriptor, K. G., Böhlke, J. K., Kraemer, T. F. and Stanton, J. S.:
642 Interaction of surface water and ground water in the Dutch Flats area, western Nebraska, 1995-99, Report, United States Geological
643 Survey. [online] Available from: <http://pubs.er.usgs.gov/publication/wri014070>, 2001b.
- 644 Welch, H. L., Green, C. T. and Coupe, R. H.: The fate and transport of nitrate in shallow groundwater in northwestern Mississippi,
645 USA, *Hydrogeology Journal*, 19(6), 1239–1252, doi:10.1007/s10040-011-0748-8, 2011.
- 646 Wells, M., Gilmore, T., Mittelstet, A., Snow, D. and Sibray, S.: Assessing Decadal Trends of a Nitrate-Contaminated Shallow
647 Aquifer in Western Nebraska Using Groundwater Isotopes, Age-Dating, and Monitoring, *Water*, 10(8), 1047,
648 doi:10.3390/w10081047, 2018.
- 649 Wheeler, D. C., Nolan, B. T., Flory, A. R., DellaValle, C. T. and Ward, M. H.: Modeling groundwater nitrate concentrations in
650 private wells in Iowa, *Science of The Total Environment*, 536, 481–488, doi:10.1016/j.scitotenv.2015.07.080, 2015.
- 651 Yonts, D.: G02-1465 Crop Water Use in Western Nebraska, University of Nebraska-Lincoln Extension [online] Available from:
652 <https://digitalcommons.unl.edu/extensionhist>, 2002.
- 653 Young, L.A. (UNL): Personal Communication with M.J. Wells, University of Nebraska, Lincoln, NE, USA, 2016.
- 654
- 655
- 656



657
 658 **Figure 1: Dutch Flats study area (A) overlain by 30 m Digital Elevation Model (USGS, 1997). The study area is located within the North**
 659 **Platte Natural Resources District of western Nebraska (B). Depending on data availability, multiple wells (well nest) or a single well may**
 660 **be found at each monitoring well location. Transect A-A' represents the location and wells displayed in the Fig. 2 hydrogeologic cross-**
 661 **section.**

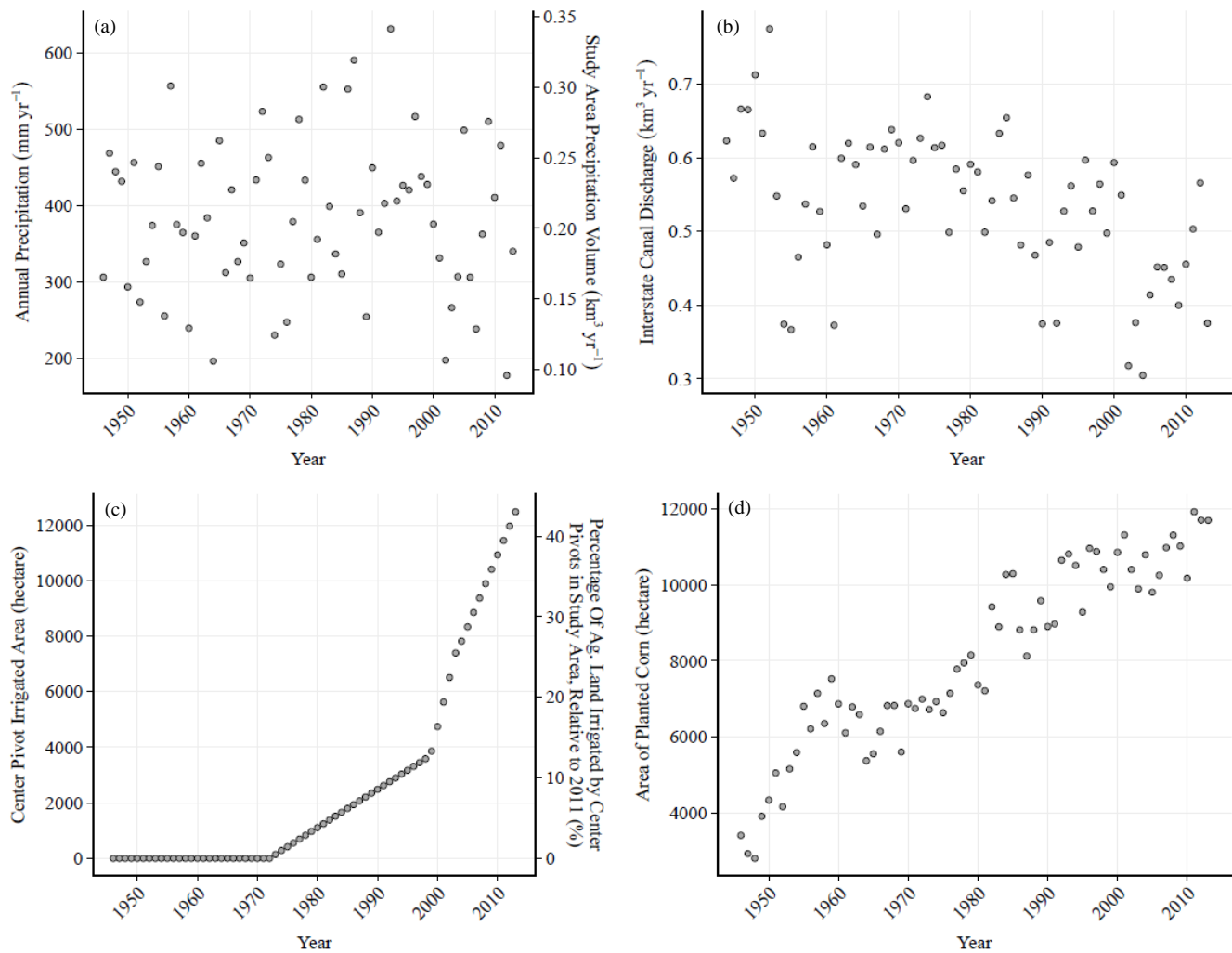
662
 663



664

665 **Figure 2: Cross-section along representative well transect (see Fig. 1) within the Dutch Flats area. Surface elevation data**
 666 **were derived from a 30-meter Digital Elevation Model (USGS, 1997). Water surface and base of aquifer elevations were**
 667 **sourced from a 1998 Dutch Flats study (Böhlke et al., 2007, Verstraeten et al., 2001a, 2001b). Small black arrows beneath**
 668 **the surface indicate general groundwater flow direction.**

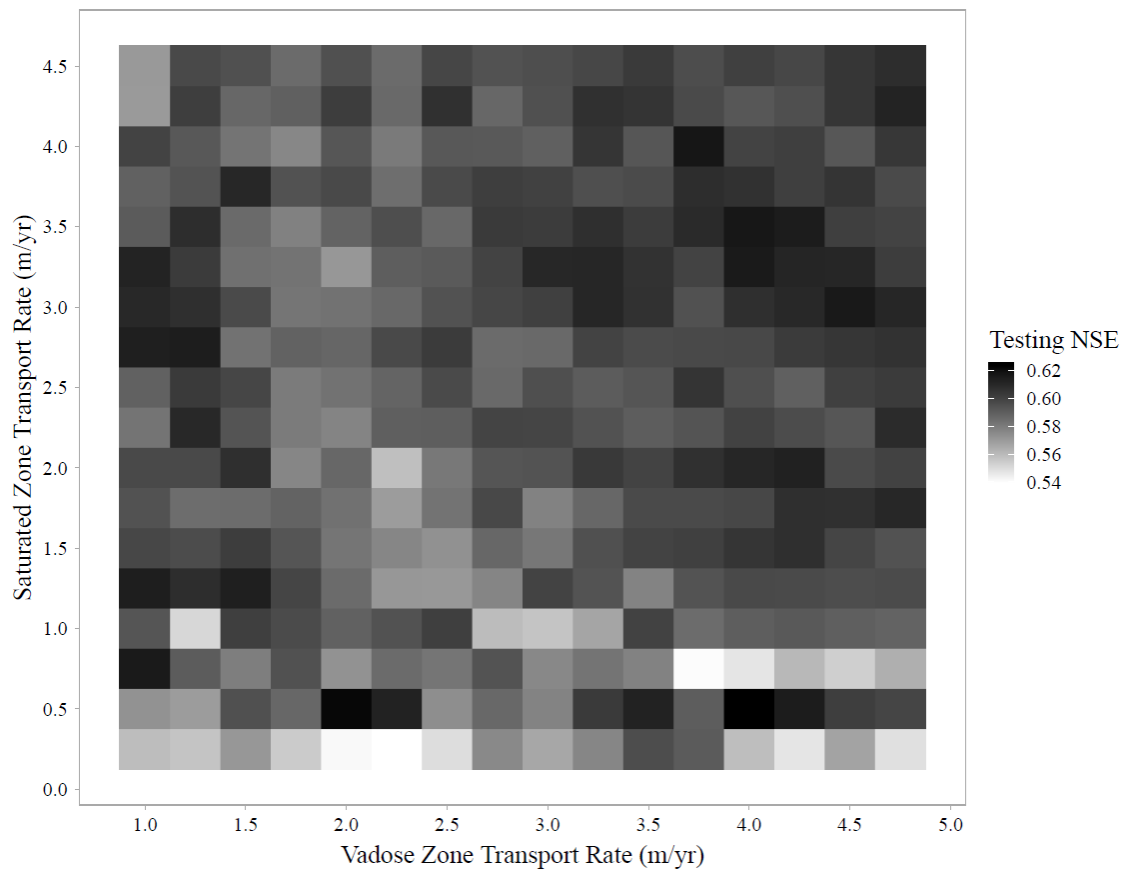
669



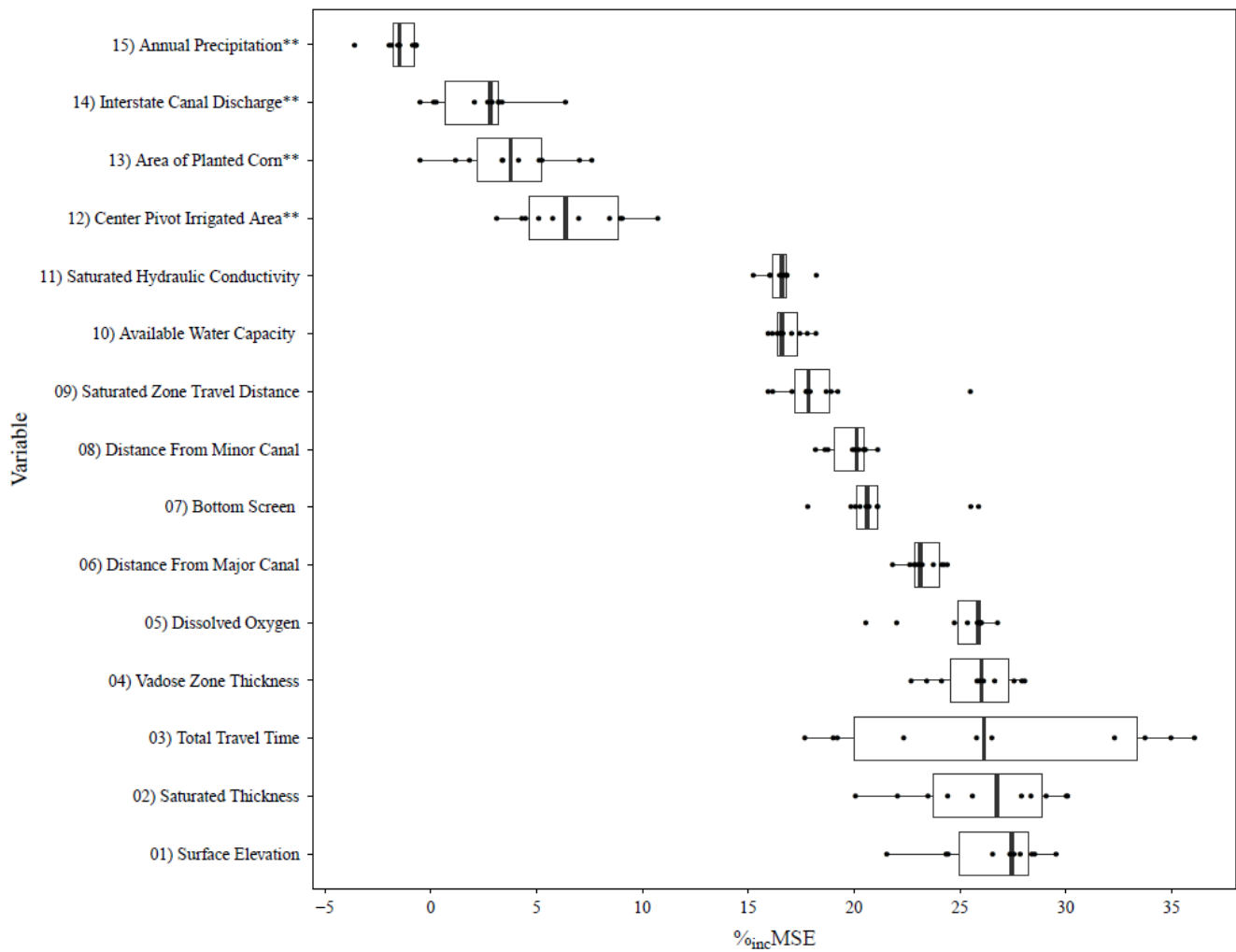
671

672 **Figure 3: Time series plots of all four dynamic predictors. Figures represent (a) annual precipitation, (b) Interstate canal discharge, (c)**
 673 **center pivot irrigated area, and (d) area of planted corn from 1946 to 2013.**

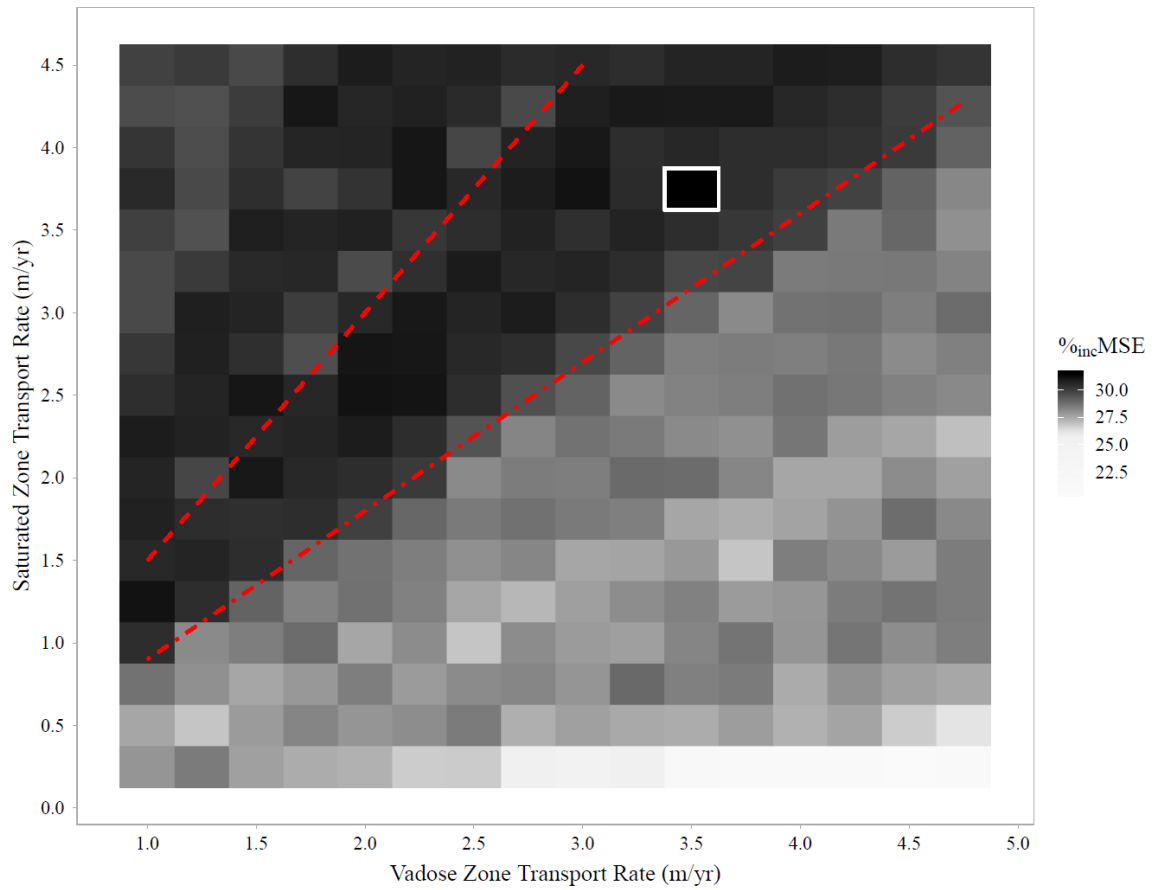
674



676
677 **Figure 4: Heat map of testing NSE results from 288 vadose and saturated-zone transport rate combinations. Testing NSE in this figure**
678 **is the median of all 25 model outputs from each of the 288 transport rate combinations. No clear pattern of optimal vadose and saturated-**
679 **zone transport rate combinations was observed.**

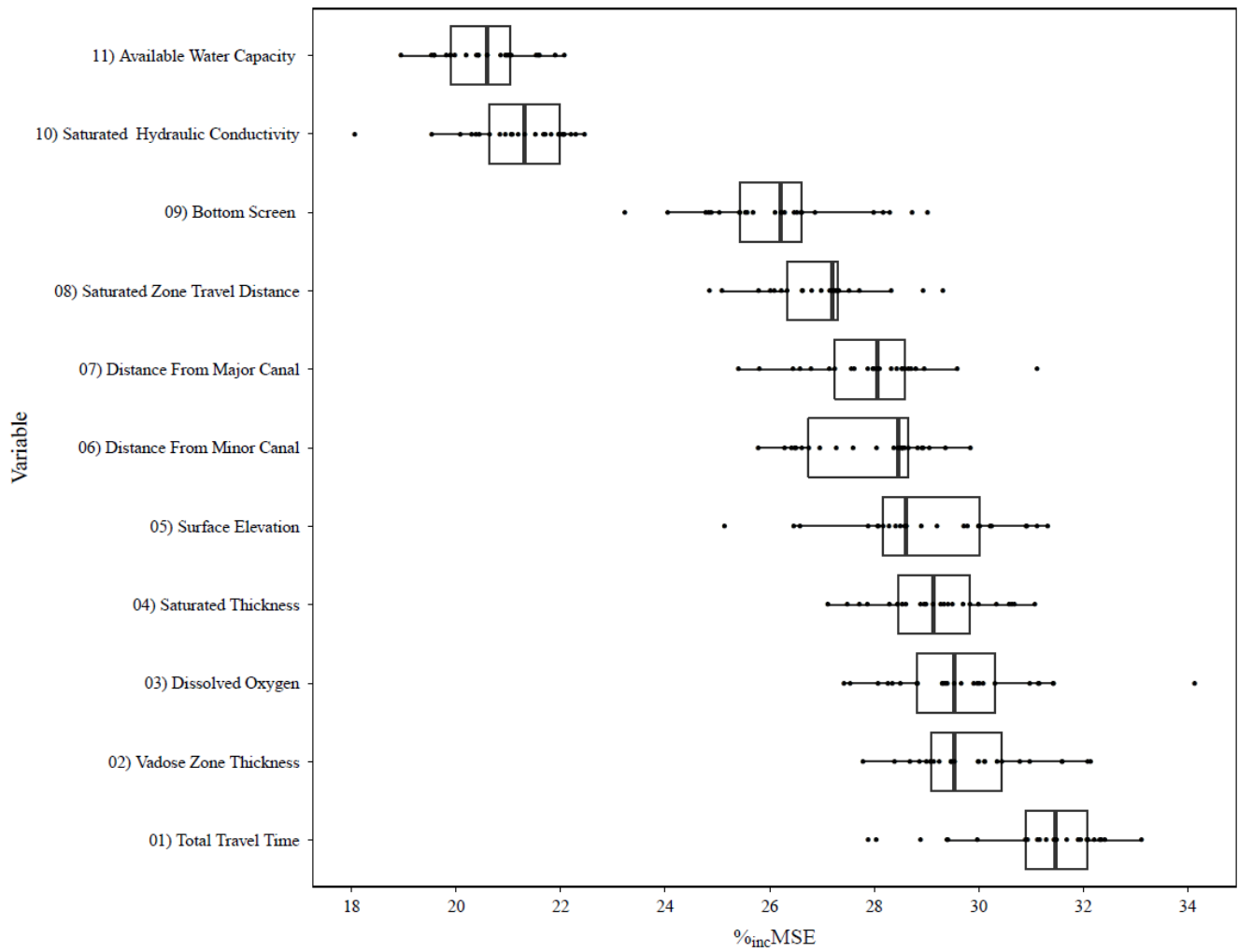


680
 681 **Figure 5: Boxplot of the %incMSE from the ten transport rate combinations shown in Table 2. Each boxplot has ten points for each**
 682 **transport rate combination, representing the median %incMSE from the 25 models (five-fold cross validation, repeated 5 times). A larger**
 683 **%incMSE suggests the variable had a greater influence on a model's ability to predict [NO_s]. **Denotes dynamic predictors.**



684
 685 **Figure 6: Heat map of %_{inc}MSE (median from 25 models) from variable importance of total travel time for each of the 288 transport**
 686 **rate combinations evaluated. Red dashed lines indicate upper ($V_u / V_u = 1.5$, long dashes) and lower (0.9, short dashes) bounds of the**
 687 **band of transport rate combinations with consistently higher %_{inc}MSE. The white square highlights the single transport rate**
 688 **combination with the highest %_{inc}MSE.**

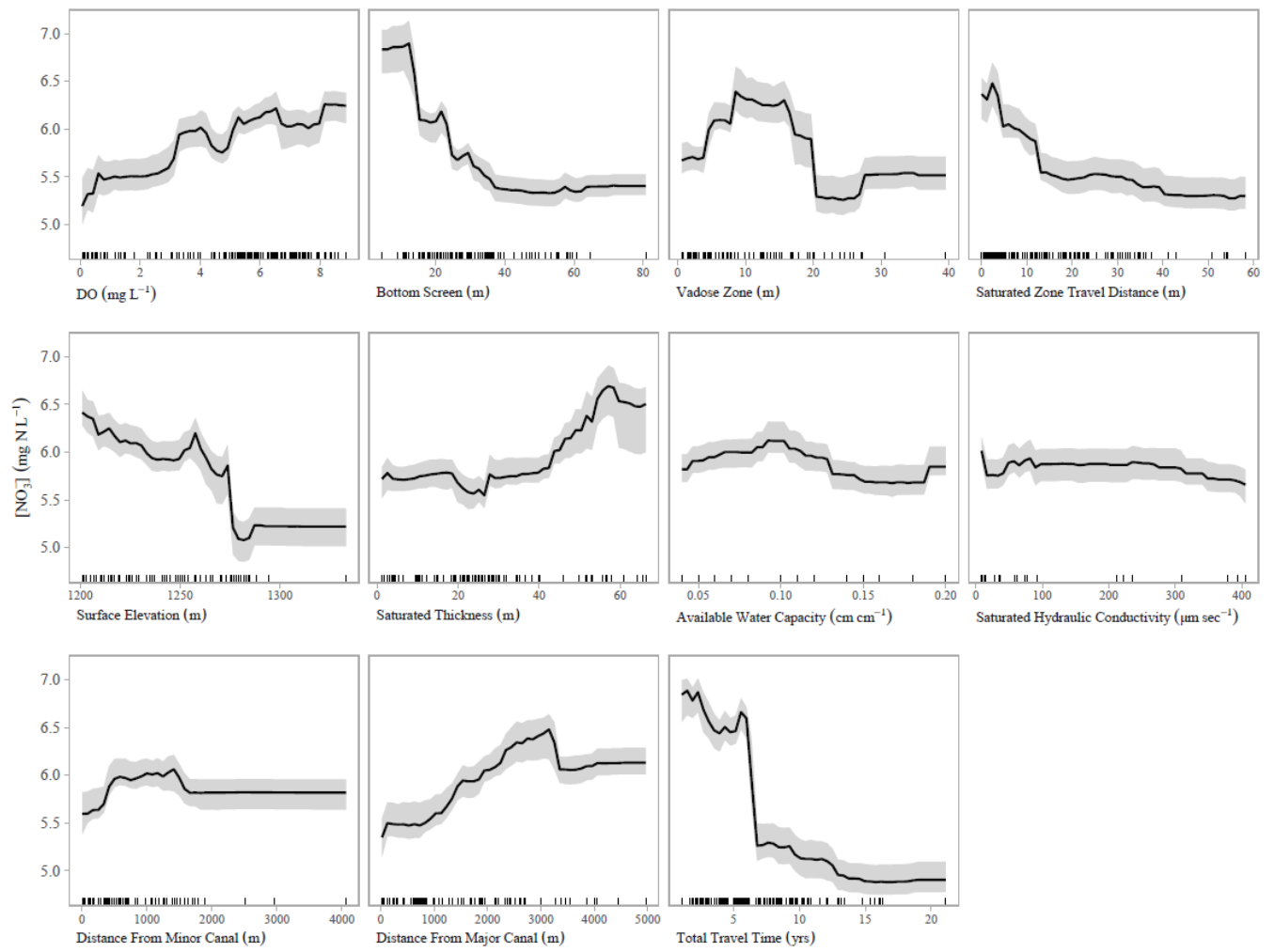
689



690
 691 **Figure 7: Plot from secondary analysis exploring variable importance of the transport rate combination with the largest median**
 692 **%incMSE in total travel time ($V_u = 3.5$ m/yr; $V_s = 3.75$ m/yr). Each point is from one of 25 Random Forest models run for this evaluation.**
 693 **A larger %incMSE suggests the variable had a greater influence on a model's ability to predict $[NO_s^-]$.**

694

695



696
 697 **Figure 8: Partial dependence plot for model evaluating transport rate combination of $V_u = 3.5$ m/yr and $V_s = 3.75$ m/yr. Tick marks on**
 698 **each plot represent predictor observations used to train models.**

699
 700
 701
 702
 703
 704
 705
 706
 707
 708

709 **Table 1. List of the 15 predictors used for Random Forest evaluation. Average (avg.) and median (med.) values are shown.**

Predictor	Units	Predictor Type	Source
Center Pivot Irrigated Area (avg. = 2618; med. = 1037) ^a	hectare	Dynamic	NAIP; NAPP; Landsat-1,5, 7, 8 ^b
Interstate Canal Discharge (avg. = 0.53; med. = 0.55) ^a	km ³ yr ⁻¹	Dynamic	USBR (2018)
Area of Planted Corn (avg. = 8065; med. = 7869) ^a	hectare	Dynamic	NASS (2018)
Precipitation (avg. = 384; med. = 377) ^a	mm yr ⁻¹	Dynamic	NOAA (2017)
Available Water Capacity (avg. = 0.1; med. = 0.1)	cm cm ⁻¹	Static	NRCS (2018)
Dissolved Oxygen (avg. = 4.6; med. = 5.4)	mg L ⁻¹	Static	C. Hudson, Personal Communication (2018)
Distance from a Major Canal (avg. = 1462.2; med. = 1161.4)	m	Static	USGS (2012) ^b
Distance from a Minor Canal (avg. = 633.2; med. = 397.6)	m	Static	USGS (2012) ^b
Bottom Screen (avg. = 26.9; med. = 24.4)	m	Static	UNL (2016) ^b
Saturated Hydraulic Conductivity (avg. = 68; med. = 28)	μm sec ⁻¹	Static	NRCS (2018)
Saturated Thickness (avg. = 30.2; med. = 27.6)	m	Static	T. Preston, Personal Communication (2017) ^b
Saturated-Zone Travel Distance (avg. = 13.3; med. = 7)	m	Static	UNL (2016) ^b
Surface Elevation (DEM) (avg. = 1244; med. = 1248)	m	Static	USGS (1997)
Total Travel Time (avg. = 6.4; med. = 5.7) ^c	years	Static	UNL (2016) ^b
Vadose-Zone Thickness (avg. = 9.9; med. = 7.3)	m	Static	T. Preston, Personal Communication (2017); A. Young, Personal Communication (2016)

^a Average and median span from 1946 to 2013

^b Data required further analysis to yield calculated values; data sources are USDA (2017) and USGS (2017)

^c Average and Median reflects transport rates of $V_u = 3.5$ m/yr and $V_u = 3.75$ m/yr

710

711 **Table 2. Summary of ten vadose and saturated-zone transport rate combinations selected from 288 unique potential combinations from**
 712 **the analysis including dynamic variables.**

	Vadose-zone Transport Rate (m/yr)	Sat. Zone Transport Rate (m/yr)	Test NSE	[NO ₃ ⁻] Observations ^a	Total Travel Time (yrs)	
					Mean (±1σ)	Median
Five Top-Performing Transport Rates	4.00	0.50	0.623	878	19.9 (± 15.8)	11.3
	2.00	0.50	0.622	861	21.6 (± 15.0)	16.5
	3.75	4.00	0.617	1049	6 (± 3.7)	5.4
	4.00	3.50	0.617	1049	6.3 (±4.1)	5.7
	4.50	3.00	0.616	1049	6.7 (± 4.7)	5.7
Extreme and Midrange Transport Combinations	4.75	4.50	0.608	1049	5.1 (± 3.2)	4.6
	2.75	2.25	0.599	1049	9.6 (± 6.3)	8.5
	1.00	4.50	0.570	1049	12.6 (± 7.7)	10.8
	1.00	0.25	0.559	607	26.7 (± 13.3)	20.6
	4.75	0.25	0.548	664	21.3 (± 15.0)	14.9

713 ^aIn cases with slow transport rates, lag times were relatively long and not all [NO₃⁻] data could be used in the model. For example, a slow transport rate combination
 714 resulting in a lag time with the infiltration year prior to 1946 could not be included. Thus, some models were ultimately based on <1,049 observations.